
**ADDIS ABABA UNIVERSITY**

**ADDIS ABABA INSTITUTE OF TECHNOLOGY**

**SCHOOL OF ELECTRICAL AND COMPUTER ENGINEERING**

**GRADUATE PROGRAM IN RAILWAY SYSTEM ENGINEERING**

# STUDY ON TECHNICAL FEASIBILITY AND DESIGN OF GRID CONNECTED SOLAR PV BASED POWER SUPPLY SYSTEM FOR THE ETHIO-DJIBOUTI RAILWAY LINE

**BY:**

**Mitiku Tilahun**

**A Thesis Submitted to the School of Graduate Studies in Partial Fulfillment of the Requirement for the Degree of Master of Science in Electrical and Computer Engineering (Railway System Engineering)**

**Advisor name:** **Dr. Ing Fekadu Shewarga**

**October, 2020 G.C**

**Addis Ababa, Ethiopia**

Submitted by:

MITIKU TILAHUN _____ _____

Student Signature Date

Approved by:

1. Dr. Ing Fekadu Shewarga _____ _____

Advisor Signature Date

_____ _____ _____

Chair or School Dean Signature Date

_____ _____ _____

Director of Post Graduate Program Signature Date

## DECLARATION

I declare that this thesis is an original report of my research entitled ‘‘**STUDY ON TECHNICAL FEASIBILITY AND DESIGN OF GRID CONNECTED SOLAR PV BASED POWER SUPPLY SYSTEM FOR THE ETHIO-DJIBOUTI RAILWAY LINE**”, has been written by me and has not been submitted for any previous degree. The experimental work is almost entirely my work; the collaborative contributions have been indicated clearly and acknowledged. Due references have been provided on all supporting literature and resources.

Mitiku Tilahun _____ _____

Student Signature Date

This is to certify that the thesis entitled, submitted by the candidate is in partial fulfillment of the requirements for the award of Master of Science degree in Electrical and Computer engineering (Railway Engineering Stream). To the best of my knowledge, the matter embodied in the thesis has not been submitted to any other University.

Advisor,

Signature Date

Dr. Ing Fekadu Shewarga _____ _____

## ACKNOWLEDGMENTS

First, I would give thanks to Almighty God for the blessing upon all of my ways and endeavors. I would like to thank my thesis advisor Dr. Ing Fekadu Shewarga at AAiT, School of Electrical and Computer Engineering upon there guidance and patience throughout the thesis work. I would also thank my sponsor DAAD and AAiT, Railway Engineering Center staff for giving the chance.

Finally, I express gratitude to my parents, friends, and colleges for providing me with unfailing support and continuous encouragement throughout my years of study and through the process of researching and writing this thesis. This accomplishment would not have been possible without them. Thank you

Author

Mitiku Tilahun

## ABSTRACT

In this thesis work the technical feasibility, design, and simulation of a single-phase grid-connected PV system is studied. The aim is to design and simulate a single-phase grid-connected PV system for railway traction applications. The design of a single-phase grid-connected PV system now days is applicable for residential, commercial, and also for large scale PV farms. To design and simulate the system, solar radiation of the site should be estimated well. Solar radiation of the site Adama, Metehara, Awash Arba, and Asebe Teferi is estimated by using temperature method and the average obtained results are 6.62 $kWh/m^2$, 7.26 $kWh/m^2$, 6.891 $kWh/m^2$ and 6.45 $kWh/m^2$ respectively. The accuracy of the estimated solar radiation values was tested by computing the MBE, RMSE, and MPE. The value of MBE and RMSE should be small as seen from the obtained results the estimated shows that the obtained value is minimum. The estimated MPE value should be in the range of (±10%) to testify the estimated value is accurate or not then, the result shows that MPE value is between in the range. The designed system to harass energy from the PV system shows that the designed power is enough to run the trainload. And also it saves 124,980.44 tons of $Co_2$ emissions during the lifetime of the project. The designed thesis will be applicable for railway traction of Ethio-Djibouti railway routes specifically around Awash Arba sections. Design will be designed and simulated by using well know software Matlab/Simulink. The design consideration for this thesis is 1 MW to run the trainload based on the technical proposal of ERC the train load is 815.4 kW.

Boosting converter is used to step-up DC voltage due to the drawback of PV system efficiency. The simple and very popular perturbed and observe MPPT method is used in this thesis works to increase solar system efficiency. This MPPT produces a duty cycle that is dependent on PV module voltage and power. The output voltage of the boost converter ranges from 1500-1600 V.

The feasibility of the designed system is studied and it takes 4.61 years of payback and which is feasible. Based on the technical proposal of Ethiopian Railway Corporation daily and annual energy consumption of the trainload is calculated and the result obtained is 3686.05 kWh and 1345.4 MWh respectively. For this thesis research energy generated from the single-phase grid-connected PV system is estimated monthly and annually and the obtained result is 884564.85 kWh and 10415.036 MWh respectively.



Key terms: Grid, MATLAB, Carbon emission, Feasibility, PV, Solar radiation, and Railway.

Table of Contents

## List of Tables

# List of Figures

# NOMENCLATURE

| | |
|---|---|
| NAMA | National Meteorological Agency |
| PV | Photovoltaic |
| COE | Cost of Electricity |
| OCS | Overhead Contact System |
| GTP | Growth and Transformation Program |
| GHG | Green House Gas |
| MW | Mega Watt |
| KW | Kilowatt |
| STC | Standard test conditions |
| PMP | Maximum rated power |
| Vin | Input voltage |
| Vo | Output voltage |
| AC | Alternating current |
| DC | Direct current |
| $\lambda$ | Duty cycle |
| A | Area of solar panel |
| $\eta_{DC, system}$ | Efficiency of DC system |
| $\eta_{AC, system}$ | Efficiency of AC system |
| $\eta_{inv, system}$ | Efficiency of inverter component |
| $\mu p$ | Number of cells connected in parallel |
| $\mu s$ | Number of cells connected in series |
| °C | Degree Celsius |
| MPPT | Maximum power point tracking |
| Isc | Solar constant |
| $\Phi$ | Latitude of the site |
| $\delta$ | Solar declination, |
| $\omega_a$ | Mean sunrise hour angle for the given month |
| n | Number of days |
| $K_i$ | Clearness index |

| | |
|---|---|
| G | Global solar radiation |
| Ge | Extraterrestrial solar radiation |
| $\Delta T$ | Change in temperature |
| $Ke$ | Empirical coefficients |
| $\delta$ | Solar declination |
| KVA | Kilovolt ampere |
| STC | Standard test condition |
| $\eta$ | Efficiency |
| $E_{dc}$ | Actual DC energy |
| Esyst | Average energy yield |
| $P_{der}$ | De rated Output power |
| PR | Performance ratio |
| $X$ | Module spacing or Row space |
| L | Length of the module |
| ß | Tilt angle and |
| $I_{ph}$ | Photocurrent |
| $I_d$ | Diode current |
| $I_{sh}$ | Shunted current |
| $N_p$ | A number of cells connected in parallel |
| K | Boltzmann constant |
| q | Electric charge |
| T | Cell temperature |
| $R_s$ | Series resistance |
| $R_{sh}$ | Shunt resistance |
| $E_g$ | Band gap energy of the cell |
| Ns | Number of series connected cell |
| $N_p$ | Number of the cell which is connected in parallel |
| $T_{op}$ | Cell operating temperature |

| | |
|---|---|
| $T_{ref}$ | Reference cell temperature |
| $I_s$ | Diode reversed saturation current |
| $I_{rs}$ | Diode reversed saturation current at operating temperature |
| $I_{sc}$ | Short circuit current |
| $V_{oc}$ | Open voltage |
| $V_{out}$ | Output voltage |
| $V_{in}$ | Source voltage |
| T | Period |
| Fsw | Switching frequency |
| ΔIL | Input ripple current |
| L | Inductor |
| C | Capacitor |
| ΔVo | Output voltage ripple |
| $P_n$ | Active power of the system |
| $\Delta I_{max}$ | Peak value of harmonic current |
| $E_n$ | RMS value of grid voltage |
| $F_n$ | Grid frequency |
| ETB | Ethiopian Birr |
| USD | United States Doller |
| BOS | Balance of System |
| $A'$ | Annual Energy Consumption |
| P | Power |
| t | Operating Time |
| k | Degree Kelvin |
| $N'$ | Total annual numbers of trips |
| PLL | Phase Locked Loop |
| ERC | Ethiopian Railway Corporation |
| PWM | Pulse Width Modulation |

| | |
|---|---|
| MBE | Mean Bias Error |
| AALRT | Addis Ababa Light Rail Transient |
| VVVF | Variable Voltage Variable Frequency |
| MPE | Mean Percentage Error |
| RMSE | Root Mean Square Error |
| GHG | Green House Gas |

# CHAPTER ONE

## 1. Introduction

### 1.1. Background of the Thesis

Solar energy is a sphere of intensely hot gas counting with a diameter of 1.39 x $10^9$ m and is, on average, 1.5 x $10^{11}$ m from the earth. Solar energy rotates on its axis every four weeks. However, it does not rotate as a solid body. The equator lasts approximately 27 days and the Polar Regions take approximately 30 days for each rotation. The temperature in the central interior regions varies from $8x10^6$ to $40x10^6$ K and the density is estimated at around 100 times that of water. The sun has an effective black body temperature of 5777K. Solar is, in effect, an uninterrupted fusion reactor with its constituent gases as the "retained container" that uses gravitational forces. Several fusion reactions have been recommended to provide the energy radiated by the sun. Electricity produced in the central solar sphere at temperatures of many hundreds of thousands of ranges must be transferred from the ground and then irradiated into space[1]. The use of useful renewable resources is increasing due to the use of the energy and distribution era.

Ethiopia is often referred to as Africa's water tower. This implies that Ethiopia has an extraordinary result for hydroelectric developments, as a consequence of the Democratic Republic of the Congo in Africa, with a potential generation of around 45,000 MW of Hydro. In addition to this, Ethiopia can generate more than one thousand MW from Geothermal and more than 10,000 MW from wind and solar energy [2]. Currently, the country's energy production depends mainly on hydro, wind, and geothermal energy, for example, the Ashgoda and Adama wind farms. However, until now, no tasks have been started to generate energy from photovoltaic energy in Ethiopia. The improvement of new sources of electricity is becoming stronger due to the essential scenario of chemical and industrial fuels, such as oil, gas, and others. The demand for photovoltaic energy has increased from 20% to 25% in the last 20 years. The market for photovoltaic structures is growing worldwide. Today, photovoltaic energy produces around 4800 GW. Between 2004 and 2009, grid-connected photovoltaic capacity reached 21 GW and was increasing at an annual average rate of 60%. To get benefit from the application of PV systems, research activities are being carried out in an attempt to gain further improvement in their cost, efficiency, and reliability [3].

There are many types of research activities conducted to use solar energy as a source of energy and support or backup for different applications. The research activities carried out are for use of residential, automobile, railway and even for air plans so, the photovoltaic system is used as a source of power and as a backup. In this research study, the only solar-powered train is considered. By mounting the solar photovoltaic system in the buildings around stations and building support structures on two sides of railway tracks or selecting a site which is nearest to the utility grid in the case of Ethio- Djibouti railway route to use as an energy source and backup for an electric train by studying solar radiation along the route area. Since the train is a level one load so, the power supply should be reliable. Here, in this research work, the selected site is Awash Arba due to more lands of free from cultivation than, which is a convent place for mounting a photovoltaic system. Since the train is level one, electricity must be reliable. As we know, the power supply includes two independent and reliable 132kV power loops for each traction substation. All AC power supply of traction substations and section posts shall adopt two 27.5kV power circuits, which are connected to the 27.5 kV bus inside the substation and of overhead contact system lines. The power feeding system of the train is from the single-phase through pantograph and is changed to three-phase by AC to DC to AC conversion mechanism to drive the asynchronous motor of the train. As we know asynchronous motor is used to drive train by using a rectifier (AC to DC convertor), single-phase input voltage is changed to DC voltage and is inverted into three-phase AC voltage by inverter inside the train locomotive [4].

This means that the generated supply system is converted into AC-DC-AC inside to supply three-phase induction motors. Already know that at the beginning 25KV is a single-phase AC and stepped down by transformer. The stepped-down voltage is converted into DC voltage and this DC voltage is filtered and protected by the DC link capacitor. And also DC voltage is inverted into three-phase AC to supply induction motor. Two inverters are connected in parallel and each inverter is connected to two to three motors. So, there may have four to six motors in a single locomotive. In the case of conversion from AC to DC to AC, DC voltage and AC voltage are controlled by control mechanisms.

This control mechanism is used to provide a variable voltage frequency and this type of power supply is feasible after the invention of a rectifier and microcontroller for the control system. Therefore, the induction motor is advantageous based on the VVVF supply system and that it uses a type of regenerative type electric brake. The inverter used for conversion from AC to DC to AC can be a voltage source inverter or a current source inverter. The conversion stages inside the train are AC voltage is step downed by the transformer, and converted into DC voltage and boosted by rectifier, DC link is used to filter harmonics from converter output and protect overvoltage. DC voltage is converted into three-phase AC voltage to supply induction motor [5]. In this research work, a grid-connected solar photovoltaic system is used to transfer extra energy into to grid after fulfilling's of local load demands and require to extract extra energy from the grid to support local load demand. The photovoltaic solar system includes a solar photovoltaic generator, a booster converter, a DC link capacitor, a single-phase inverter, a low pass filter, a transformer, and a grid supply connected to form a grid-connected solar photovoltaic system. Grid interconnection of a solar PV system is carried out by the inverter, which converts DC voltage generated from PV array to AC voltage to supply AC electrical materials. The produced output voltage must be synchronized and in phase with the grid, the voltage to get output free of harmonics [6].

## 1.2. Photovoltaic Array

A photovoltaic system is made up of several photovoltaic cells. A small PV cell is generated 1 or 2 W of power and depends on the type of material used. To generate higher power PV cells can be connected in series or parallel to form modules. Depending upon power generation the group of modules connected to form PV array. PV array is interconnected with a boost converter, inverter, and transformer to generate power and supply energy to the load [7]

### 1.2.1. Photovoltaic Characteristics

The photovoltaic cell consists of two or more thin layers of semiconducting material most commonly silicon. The photovoltaic cell is composed of several semiconductors and only a moderate conductor of electricity. The most commonly used materials are silicon (Si), cadmium sulfide compounds (CdS), and gallium arsenide (GaAs). When the silicon is exposed to sunlight, the electrical charges are generated and directed by the metal contacts as indicated (DC). The electrical output of a single cell is small and to increase the output we need to connect more cells

in parallel and series, and they are known as photovoltaic modules. Once again to increase the output, we will connect the photovoltaic modules in parallel and series and known as photovoltaic arrays. Photovoltaic panels are devices that convert sunlight into electricity without requiring any motor or rotating equipment. It generates electricity without emissions and its operation is silent [8]. Ethiopia is located near the equator at latitudes of 3 ° and 15 ° north and 33 ° to 48 ° east with a moderate influence of temperature and a pleasant climate. In this study, Awash Arba is selected and the site is located in the eastern part of the country with a latitude of 11.756 degree, longitude 40.960 degree, and an altitude of 986 m.

## 1.3. Statement of the problem

One of the main needs of socio-economic development in any country of the world is the provision of reliable and clean energy supply systems. In recent years, there is considerable growth in the use of renewable energy resources worldwide, and in the local markets are observed. In particular, solar energy is site-dependent, non-polluting, and high potential sources of alternative energy production. The solar PV system is essential for the development of the green economy of any country and reduces carbon dioxide emissions in the region. It is known that the development of any country depends on the amount of energy consumption. Which is well know that, energy consumption is proportional to economic development. The per capita energy consumption in Ethiopia is very low and depends mainly on hydropower and biomass. But, the construction and production of hydropower have a high initial cost. And, in recent years because of the drought, the flow of water in the dams is extremely decreased. For example, in each winter season, Tesabay I and II almost zero or less electricity, and Tekza's hydropower energy production in the last years has been decreased due to the drought case. Therefore, the renewable source of energy is a promising way to compensate for this kind of problem and also pollution-free and environmentally friendly. By considering these initial aspects doing this research is very interesting and, in this design consideration as supply and as a backup for the electric train through the solar system (PV) in the case of the Ethio-Djibouti route, by installing photovoltaic systems on both sides of the railway line and the rooftop of the stations or selected site.

## 1.4. Related Works

The application of solar energy for the railway is limited due to the lack of advanced technologies, but some countries plan to use the system for different uses in their railway system. S. Ali. et al (2010) studied the feasibility of a solar-powered railway system for light urban transport in Pakistan to compare rail systems based on existing fuel with a photovoltaic system [9]. The Indian railroad plans to, greening the tracks to achieving the one Gigawatt photovoltaic plant as an energy source for railway locomotives by installing a photovoltaic solar system on railway coaches and rail lines[10]. L. Alboteanu. et al (2006) studied the employment of photovoltaic energy for lighting railways by evaluating the electrical demand of each train using the HOMER software[11]. Kezuka, H. K. T and et al studied the solar light rail train at the Tokyo University of Technology[12]. In the case of our country, Shimels, K. (2015) studies the design of a hybrid solar-fuel energy system for the application of the locomotive train power source for the AALRT and Ethio-Djibouti routes. In this study, a photovoltaic system in rail cars are proposed to install, but there may be power interruption due to cloudy days and season of some route, influence on the lifetime of the photovoltaic system due to irregularities movement and a load of PV influence lifetime of the train in the railway tracks[13].

## 1.5. Scope of research work

Before development of this thesis work and proposal, the grid-connected photovoltaic system in the railway track line had not designed and installed. Therefore, the grid-connected photovoltaic system installed near to railway stations around Awash Arba is used to support the national grid as an energy source and as backup power for electric train locomotives.

## 1.6. General objectives

The major objective of this research is to study technical the feasibility and design of the solar photovoltaic system as an energy source and backup for the electrification of the electric train by installing a photovoltaic solar system near to the stations of the railway tracks line around the railway line Awash Arba of Ethio -Djibouti railway route to develop green energy strategies.

### 1.6.1. Specific Objectives

The specific objective includes the following goals:

- ✓ Collecting metrological data for selected sites.
- ✓ Determining solar radiation of selected sites from collected meteorological data.
- ✓ Computing the amount of solar energy from computed solar radiation of selected sites.
- ✓ Developing system design for a solar PV system by using sensitivity tool software.
- ✓ Estimation of the solar photovoltaic potential and cost analysis for the given route.
- ✓ Economic evaluation and compare its feasibilities.
- ✓ Developing a computer model for system integration of solar PV system and existing electric traction system with the national grid.

## 1.7. Significance of Research

At the end of thise research, the design and simulation will expected and works well, feasibility is studied, and designed grid-connected solar photovoltaic system would be connected to supply electric train in case of Ethio- Djibouti railway line and the electric train will get environmentally friendly and interruption-free supply system. Grid-connected photovoltaic system supply will be near to Awash Arba (Sebat) stations of railway tracks line in the route of Ethio- Djibouti railway line.

## 1.8. Research Questions

In this part of the research proposal, some questions will be answered after the completion of this research. These research questions have been formulated below.

- ❖ What are the issues and challenges of the existing railway line from the power supply system's point of view?
- ❖ What are the possible ways to eliminate this issue in our railway lines specifically for Ethio-Djibouti railway lines?
- ❖ Is it feasible to supply an electric train solar PV system?
- ❖ How and when it works as backup and a power source for electric trains?
- ❖ How much it's functional to eliminate possible issues in our energy demand of electric train locomotives?

- How that installed solar PV system is inspected and monitored to get efficient, uninterrupted and the exact amount of power supply system to our electric train in every day to day operations?

## 1.9. Thesis Work Organization

This thesis is organized into the six chapters, the first chapter contains the introduction of solar energy, the second chapter contains a literature review, the third chapter contains the study of technical feasibility and design and simulation of the grid-connected PV system, chapter four contains control strategies of the designed system, chapter five contains cost estimation and chapter six contains results, conclusion, and recommendation and at the end of thesis work reference is included.

### 1.9.1. Research Methods, Materials, And Procedures

The methodologies followed in this study are reviewing different kinds of literature, collecting data, modeling, and analyzing solar radiation of the sites for solar (PV) systems, design, and simulation of solar (PV) system by using MATLAB software as a sensitivity analysis tool to be used.

### 1.9.2. Data Collection and Literature Survey

Data will be collected from different organizations and agencies like the National Meteorological Agency. Minimum and Maximum temperature of the site will be collected from these organizations and agencies. Geographical layout, surrounding environment concerning the design of the solar (PV) system will be collected by visiting the sites. And also another source of data will be collected from different websites, especially related to the cost of PV modules, converter, and regulator.

Related literature on railway electrification by solar (PV) systems from Ethiopia and other countries will be considered. These include papers, journals, books, and related sources to electric train load estimation, potential assessment techniques of solar resources for research.

# CHAPTER TWO

## 2. Literature Review

The use of renewable energy resources is increasing from time to time throughout the world to generate energy through harassment such as wind, heat, and solar energy. In this research work, solar energy is selected to generate electricity from sunlight, which is abundant throughout the world. When designing a solar energy system, knowledge of monthly global solar radiation is essential. Many scholars have used different models to determine the global solar radiation of the site, among those a few models are analyzed below. Over the years, several researchers have used many types of models to determine global solar radiation in different corners of countries from various meteorological parameters such as air temperature [14],[15], sun (Angstrom and Prescott), Perception, relative humidity, and cloudiness. E. Quansah and et al studied the empirical model of air temperature estimation. In their study, they analyzed the performance of both sunshine and air temperature and the estimated value is compared with the measured value of the global solar radiation of the different sites of Ghana. The measured and estimated global solar radiation is a very good agreement and the coefficient of determination varies from 0.88 to 0.96. The estimated value compared to the measured value is checked by MBE, MPE, and RMSE with a very small value. A.Q. Jakhrani and et al. [16] estimated global solar radiation by using sunshine and other meteorological parameters. Those researchers estimated the global solar radiation by different methods, like sunshine hours, temperature method, and other meteorological parameters. Based on this research, the researchers compute and compare the global solar radiation of sites and the research of these researchers when they stated that the results of the proposed model, RMSE, and MBE are acceptable.

Richard G. Allen. [17] Studied the self-calibrating method for solar radiation from air temperature. On these works, scholar uses a simple and conservative approach and, in this study, the empirical coefficient approach is used to determine the global solar radiation of the site Kr = 0.16 for the interior locations and Kr = 0.19 for the coastal regions. In this estimation, the finding of global solar radiation is well determined and the scholar compared and analyzed by calculating a standard estimation error (SEE). Sarsah, E. A. and Uba, F.A. [18] They proposed another model which is called the angstrom method. The model is used to determine the monthly global solar radiation of

the site. This type of study is especially useful for remote locations and the site which is not under measurement of the national meteorological agency of the country. In their study, the Angstrom-Prescott model of the sunshine method is used and estimated for each month. They reach a good agreement by using different regression equations for each month and they take the best for all the months. Many researchers have studied the feasibility of solar radiation in different locations of Ethiopia and they concluded that the country has enough solar radiation to install and operate the solar plant. Among the researchers, N. Argaw [10] Presented the estimation of solar radiation in different sites of Ethiopia, such as Addis Ababa, Bahir Dar, Nedjo, and Zeway. The solar radiation estimated at these sites varies between 4.13 $kW/m^2$ /day and 6.62 4.13$kW/m^2$ /day. The estimation is based on the Angstrom regression models of sun hour. Sharew A. [11] Studied the solar potential assessment in Ethiopia by using two different methods. According to his estimation, he uses a simple model of radiative transfer of the atmospheric pressure of the sun whose minimum value is 17.42$MJ/m^2$/day or 4.78 4.13$kW/m^2$ /day in December in Gonder and maximum value 23.66MJ/ m2/day or 6.52$kWh/m^2$/day. He presented that the monthly global solar radiation on the horizontal surface is approximately 12$MJ/m^2$/day according to the prediction of the vapor pressure radiation model and 19.5$MJ/m^2$/day according to the simple model of atmospheric pressure radiative transfer of sunshine model prediction. Shimles K. [12] Estimated of solar radiation on the railway routes of AALRT and Ethio-Djibouti by using the old known Angstrom correlation method. He presented and concluded that the monthly global solar radiation distribution of railway lines with minimum value of 4.37 $kWh/m^2$/day in August in Addis Ababa and the maximum value of 7.24 $kWh/m^2$/day in May in Dire Dawa. In the above estimation and studies, the country has abundant solar energy to install a photovoltaic solar system. Studies indicates that the country has an average monthly global solar radiation of 5.87 $kWh/m^2$/day.

Know that Ethiopia is located around the equator and the country has almost equal day and night and moderate air temperature throughout the year when compared to that of the North and South Pole.


Figure 3. 1 Locations of Ethiopia in the world map

## 2.1. Grid-Connected Solar PV System for Different Applications

Due to the shortage and environmental pollution of fossil fuel during exhausting opens the eye to see the alternative energy source. Among those of many energy sources, solar energy is a clean, inexhaustible, silent, and environmentally friendly renewable energy source. Either PV system or another renewable energy source may not continuously supply energy due to seasonal variations so, a grid-connected energy system is a nowadays promising way to supply energy continuously.

Grid-connected solar photovoltaic system power generation is more advantageous than standalone due to the effective utilization of generated power. A grid-connected PV system may be a single-phase or three-phase depending upon their application. While for this research work single phase is considered because the power supply of the Ethio-Djibouti railway is single phase 25 kV. The

grid-connected PV system is now a day adopted from small to higher power usage for residential use, commercial use, and utility use. Many scholars have studied the grid-connected PV system and standalone PV system for different use. For this thesis work, a grid-connected solar PV system will be considered for the electrifying railway of Ethio-Djibouti railway routes. The site for the photovoltaic system installation will again be considered from Ethio-Djibouti routes of one section which is from Meiso to Awash Arba (Sebat) due to the free space that exists near to the stations. The selected site in my consideration is good land topography and again not used for any use, leveled and it may not need more evacuation during land preparation for photovoltaic system installation and the solar radiation for this site is a great value from winter to summer. Out of 67 GWP PV installed globally, 80% is the grid-connected type. D.B. Raut and A. Bhattrai [19] proposed the system which analyzes the performance of the grid-connected system by using Matlab/Simulink, in which the performance of the grid-connected system drop off due to irradiance levels are decreased and the nonlinear devices used in the converter circuits are a source of harmonics.

R. Verma and Prof. K. Gupta [14] designed and simulated a grid-connected PV system with the practice of harmonics compensation by using MatLab Simulink to supply electricity for different applications like to control residential appliance, business instrumentality electricity, lightning for all the kinds of building.

M. S. Hassen and A. A. Elbaset [20] studied a comparative study for the optimum design of grid-connected solar PV system installation on institutional buildings at the University of Minia, Egypt. In which the system is based on the new approach of configurations of the solar PV system with inverter and without MPPT by using the MatLab simulation approach. This results in annual energy production of about 258.8 MWh, COE of about 0.5482 $/kWh, payback period equal to 6.95 years, and total annual GHG emissions reduction of about 180.9 tons.

Jasim A. [16] At the University of Diyala, Iraq designed a solar off-grid PV system to supply the electricity for a residential unit. The average daily load of the selected residential unit is 36 kWh/day then, the load requirement of the design was met by 44 solar modules.

From many scholar's studies, a grid-connected solar PV system is used for railway applications and commercial use. F. Ciccarelli and R. Rizzo [21] Proposed the control techniques and optimal storage devices to improve the performance of tramways by using energy storage systems. This

study analyzes the integration of power plants, supercapacitor energy storage system, and existing railway power system. D.Gowda, S.S. Lokare, and et al [22] Studied on the modifications of the solar train to use solar PV system to store energy in the battery to reduce the extenuation. By analyzing the power consumption of one train bogie. In this study solar panels and batteries are on the train coaches so, it may have some additional loads. M.S.Vasisht, G. A. Vashista, and et al [23] Studied the feasibility of a rooftop solar photovoltaic system on railway coaches. Based on the result one rail coach generates at least 18 kWh of electricity in a day which saves 1700 liter of annual diesel consumption and reduces carbon dioxide emission by 45 tones in each coach per year. But still, the solar PV system is in the rail coach then, it may affect the rail track and PV system lifetime due to irregularity of the train movement.

# CHAPTER THREE

## 3. Study on Technical Feasibility and Design of A Grid-Connected Solar PV System

The government of Ethiopia wants to solve the transportation problem in different ways like by using railway and expressways. Government plans to build more than 5000 km in different corners of the country during GTP I and GTP II to overcome transportation problems and increase export and import of commodities in every corner of the port route in a short period. Because of the lack of transportation means the farmers can't address their product to the customer, industries and there is transportation problem to get raw material in time and import and export of produced products and takes a long time to reaches to the market so, because of this the end-users are going to pay the additional cost. To overcome this problem the railway transportation is crucial. The Ethio-Djibouti railway line is one of the routes to overcome the challenges of import and export of the products and to provide the cheapest and safe transportation opportunity to the customer.

This rail route has both freight and passenger trains to transport goods and passengers from Addis Ababa to Djibouti port route. Railway lines cover many small and big towns of the country such as Debere Zeit, Natherat, Mieso, Awash Arba (Sebat), Metehara, and Dire Dawa. To build a railway line some basics will be taken into considerations. Those are the topography of the line, import and export capacity of the country, passenger flow in the route, and electric supply access and the amount will be considered. The electric supply system for rail routes should be easy to manage, safe, reliable, and economical, easy to maintain, and flexible in operation mode. The Ethio-Djibouti railway line uses the electric supply system generated from hydropower, wind, and diesel as a source and backup system. The power supply system for cross country (Ethio-Djibouti) is a single-phase AC 25 kV, a 50 Hz direct feeding system with a regenerative braking system (return wire) is applied. The design and distribution of the power supply system should be meet the requirements and capacity of the trainload. The traction substation is temporarily powered by 132KV voltage and types of traction transformer used in the railway route are Vv single phase transformer from Sebeta to Mieso and Vv three-phase transformer for the rest of route. The electric traction substation with Level-1 load will be supplied by two independent and reliable 132 kV power sources and to improve the reliability of the external power supply of traction substation is

recommended that external power sources of each traction substation come from different substations or buses of different sections in the same transformer substation.

The voltage of the overhead contact system (OCS) shall be as follows: nominal voltage which is 25 kV, a maximum working voltage of 27.5 kV; minimum short-time voltage of 29 kV, the minimum working voltage of 20 kV and working voltage under abnormal conditions is 19 kV. Nearly as we know that our country mostly depends on hydropower and fossil fuel to power the loads but, fuel is nonrenewable and pollutant to the environment and due to seasonal change most of our dams in the winter season of Ethiopia is dramatically decreased like Tese Abay I, II and Tekeze almost zero power during this season. To compensate for this, increase the country's power generation and, to prevent the environment from the pollution other options should under consideration like Sun, Wind, and Geothermal which is a renewable resource. In this thesis, the solar energy is selected to generate and supply the trainload and the selected system is a grid-connected solar photovoltaic system. The load of the Ethio-Djibouti railway line depends on the train type used in the route. The load for electric-type car the maximum load is 815.4 kW and for diesel type cars the maximum load is 1840 kW. So, to accommodate electric type train load with 815.4 kW power in this research work 1 MW will be considered and generated from the photovoltaic system will easily manage the loads in the route. According to the technical proposal of the Ethiopian Railway Corporation (ERC), a different type of railway locomotives are proposed. The proposed train differs and grouped based on the type of power sources, the purpose and capacity of train cars. From the technical proposal of ERC trains are used for both passenger and freight purpose and type of train locomotives used are YZ25G for passenger, Boxcar for freight, and DFN7G for multipurpose which is diesel type.

**Technical specification of train locomotives**

Table 3. 1 Specification of proposed train types for Ethio-Djibouti railway

| Locomotive parameter | Boxcar | YZ25G | DFN7G |
|---|---|---|---|
| Purpose of locomotive | Freight | Passenger | Multi-purpose |
| Length(mm) | 17400 | 25500 | 18800 |
| Width(mm) | 3105 | 3105 | 3300 |
| Power Source | Electric-DC600V | Electric- DC600V | Diesel-electric DC770 |
| Voltage rated(V) | 600 | 600 | 770 |
| Rated current(A) | 1359 | 1359 | 2389.61 |
| Fuel consumption at rated power(gm) | - | - | 207+3%g/kWh (469062gm) |
| Operating temperature | -40 to 40 $^0$C | -40 to 40 $^0$C | -20 to 500$^0$C |
| Max. configuration of car in train | 20 | 20 | 20 |
| Roof top area of each locomotive($m^2$)/car | 54.027 | 79.1775 | 62.0 |
| Effective area of locomotive ($m^2$)/car | 50 | 70 | 58 |
| Total effective area( $m^2$) | 1000 | 1400 | 1160 |

## 3.1. Design and Simulation of the Grid-Connected Photovoltaic System

In this thesis work, solar radiation of the sites will be estimated first, and the design and simulation of a system for a single-phase grid-connected photovoltaic system will be designed and simulated by using MATLAB/Simulink and proceeded to the next chapter. Before designing and simulating any solar PV energy system solar radiation should be estimated and the feasibility of the system will be studied well. Once solar radiation is determined and the estimated, solar radiation is feasible to generate the power, and design and simulation of a solar PV system to supply energy to the load. Any photovoltaic system design depends on the capacity, size, and type of load demands of the end-user. We know that our load here is a train locomotive having load profiles discussed before. In this thesis single-phase grid-connected PV system is considered and contains components like PV array, DC to DC (Boost) converter, DC link capacitor, DC to AC inverter, filter, transformer, and the utility grid. PV array is used to convert sunlight into electricity through photovoltaic effect and array is composed of solar modules and again modules are composed of solar cells. The boost converter is used to transform DC voltage from one level to another higher DC voltage according to train supply specification[5]. This will be done by varying the duty cycle of the converter by using the MPPT algorithm. DC link capacitor is used to connect the converter and inverter and reduce high-frequency harmonics. The single-stage inverter is also used to convert DC into AC to supply alternating current loads. The inverter is also selected and designed based on the train supply specification. The filter is also used to decrease harmonics from inverter output and wave shaping purpose which means the output of the inverter is square wave while we need for our load the sine wave. The shape of the inverter output voltage is a square wave then by using a low pass LCL filter we can convert this square wave into a sine wave and which is in phase with the grid voltage. The transformer is used to step down or up the generated voltage from the PV array and utility grid to supply the trainload. Normally the system is transformerless which means the transformer is embedded into the train coach and the specification is already known from the beginning. The utility grid is single phase 25 kV, 50Hz which is standard for traction of train loads.

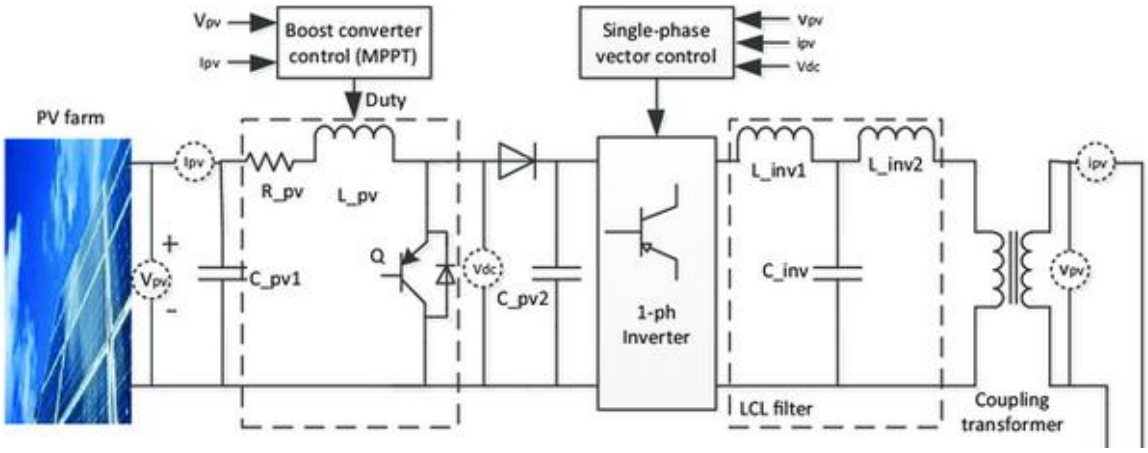


Figure 3. 2 Grid-connected PV system diagram

From the technical proposal of Ethiopian Railway Corporation, the maximum load for the electric type of load is 815.4 kW so, to accommodate the load in this thesis generated power will be more than 815.4 kW and let us consider 1 MW to supply all auxiliary power system.

## 3.2. Estimation of Solar Radiation

Solar radiation is the primary source of energy for the Earths. Solar radiation plays an important role as a renewable energy source and is used to estimate potential power levels that can be generated by photovoltaic cells. Solar radiation is also useful for many applications such as agriculture, evaporation, atmospheric, land, and oceans[7]. There are different models used to estimate global solar radiation based on different available meteorological data. The followings model are categorized below: Cloud-based, sunshine duration based, rainfall-based, and temperature-based. Among those of different models in this thesis study temperature-based model is considered to estimate solar radiation of the selected locations. Model is explained as follows: The measured monthly average daily global solar radiation, maximum and minimum temperature of the study area is from the National Meteorological Agency or NASA. For this study, the meteorological data covers six years of temperature record from 2011 to 2016 of the sites listed below. The latitude, longitude, and altitude of the selected site above sea level are given in the table below.

Table 3. 2 Latitude, Longitude, and Altitude information of the selected location

| No. | Site | Latitude (℃) | Longitude (℃) | Altitude (meter) |
|---|---|---|---|---|
| 1 | Adama | 8.526 | 39.2583 | 1712 |
| 2 | Metehara | 8.90 | 39.9170 | 947 |
| 3 | Awash Arba | 11.756 | 40.958688 | 986 |
| 4 | Asebe Teferi | 9.08 | 40.8652 | 1826 |

To estimate solar radiation of the selected site first extraterrestrial solar radiation is determined ,and calculated as follow:

Extraterrestrial solar radiation is the maximum amount of solar radiation available to the earth at the top of the atmosphere[24]. The monthly average daily extraterrestrial radiation on a horizontal surface (*Ge*) can be calculated for average days of each month from the following equation.

$$Ge = \left(\frac{24}{\pi}\right) Isc \left[1 + 0.033\, cos\left(\frac{360n}{365}\right)\right]\left[\begin{matrix} cos\phi\ cos\Theta sin\omega a \\ +\left(\frac{2\pi\omega a}{360}\right) sin\phi\ sin\Theta \end{matrix}\right] \quad 3.1$$

Or

$$let, A = [cos\phi\ cos\Theta sin\omega a + \left(\frac{2\pi\omega a}{360}\right) sin\phi\ sin\Theta] \quad 3.2$$

$$Ge = \left(\frac{24}{\pi}\right) * Isc \left[1 + 0.033\, cos\left(\frac{360n}{365}\right)\right] * A \quad 3.3$$

Where, $I_{sc}$ is solar constant (1367 w/m$^2$), ϕ is the latitude of the site, Θ is solar declination, $\omega_a$ is the mean sunrise hour angle for the given month and n is the number of days of the year starting from the first January to 31$^{st}$ of December. Then, solar declination (Θ) and the mean sunrise hour angle ($\omega_a$) can be calculated by the following equation:

$$\Theta = 23.45\, sin\left[360\left(\frac{284 + n}{365}\right)\right] \quad 3.4$$

And

$$\omega_a = \cos^{-1}(-\tan\phi\ \tan\Theta) \quad 3.5$$

The clearness index ($K_i$) is defined as the ratio of the measured (Observed) horizontal terrestrial solar radiation G, to the calculated (predicted or estimated) horizontal extraterrestrial solar radiation $G_e$.

$$Ki = \frac{G}{Ge} \quad 3.6$$

The clearness index (Ki) gives the percentage deflection by the sky of the incoming global solar radiation and therefore indicates both levels of availability of solar radiation and changes in atmospheric conditions in the given locality.

Then, Ge can be calculated from the data whereas G is global solar radiation calculated by the formula given below.

Hargreaves and Samani developed an empirical model that took the relation between the relative incoming solar radiation and the square root of the temperature differences.

$$\frac{G}{Ge} = Ke(\ \Delta T)^{0.5}) \quad 3.7$$

$$G = Ge\big(Ke(\ Tmax - Tmin)^{0.5})\big) \quad 3.8$$

Where, $\Delta T$ is the average monthly change in temperatures. $K_e$ is empirical coefficients but according to Hargreaves's recommendation *Ke* is equal to 0.16 for interior regions and *Ke* is equal to 0.19 for coastal regions.

So, by substituting the value of empirical coefficient *Ke* the monthly global solar radiation of the sites can be determined [8]. The units of in kWh/m$^2$/day is converted into MJ/m$^2$/day using a factor of 3.6 proposed by Hargreaves and Samani.

Based on the temperature model, Hargreaves and Samani suggested that the clearness index *Ki* is equal to monthly average daily extraterrestrial radiation on a horizontal surface (Ge) to global solar radiation (G) would be estimated by using the following formula:

$$\frac{G}{Ge} = \xi(\Delta T)^{0.5} \quad 3.9$$

Where, G is global solar radiation, Ge is monthly extraterrestrial solar radiation, $\Delta T$ is changed in temperature (Tmax minus Tmin) and $\xi$ is a dimensionless empirical parameter which is 0.16 for interior regions and 0.17 for coastal regions[25]. By considering those all selected sites $\xi$ for interior regions is which equal to 0.16.

By considering the influence of altitude $\xi$ is estimated by using:

$$\xi = \xi o \left( \frac{P_a}{Po} \right)^{0.5} \quad 3.10$$

Where: $P_a$ and Po are the average atmospheric pressures at the altitude of the place and sea level respectively and αo was 0.17 for interior regions and 0.2 for coastal areas. Later Chadel et al proposed a new model based on latitude functions to determine αo then:

$$\xi o = (\Phi)^{-1}(\sin \Phi)^{0.5} \quad 3.11$$

Where, Φ is latitude

Using all the above formula we can determine extraterrestrial radiation and global solar radiation.

As shown below one month's extraterrestrial radiation and global solar radiation is determined from the given parameters as follows: Solar declination (δ) and the mean sunrise hour angle ($\omega_a$) can be calculated by the following equation for the first months (January) n is the number of days equal to 31 for January months of the year [7].

$$\theta = 23.45\, sin[360\left(\frac{284 + n}{365}\right)]$$

$$\theta = 23.45\, sin[360\left(\frac{284 + 31}{365}\right)]$$

$$\theta = -17.78$$

Sunrise hour angle for the January months is calculated as follows:

$\omega_a = \cos^{-1}(-\tan \phi \tan \theta)$

$\omega_a = \cos^{-1}(-\tan 8.526 \tan -17.78) = 92.75^0$

Where, $\phi$ is the latitude of the site Adama (Natherat).

$\omega_a = \cos^{-1}(-\tan \phi \tan \theta)$

Then, extraterrestrial solar radiation of the site is determined by the following formula:

$$Ge = \left(\frac{24}{\pi}\right) Isc \left[1 + 0.033 \cos\left(\frac{360n}{365}\right)\right]\left[cos\phi\, cos\theta sin\omega a + \left(\frac{2\pi\omega s}{360}\right) sin\phi\, sin\theta\right]$$

For n=31, $\phi = 8.526$, $\theta = -17.78$, $\omega a = 92.75^0$ and Isc=1367 w/m$^2$

$$\text{Ge} = \left(\frac{24}{\pi}\right) * 1367 \left[1 + 0.033 \cos\left(\frac{360 * 31}{365}\right)\right]\left[\cos(8.526)\cos(-17.78)\sin(92.75) + \left(\frac{2\pi * 92.75}{360}\right)\sin(8.526)\sin(-17.78)\right]$$

Then, Ge=9.297 kWh/m$^2$/day

For the rest of the months, solar radiation is calculated in the same procedure but, the number of days n's is the sum of the current month's day plus the previous month's day and the result is listed table below for the six consecutive years of minimum and maximum temperature distribution of location. Then, from Hargreaves and Samani's empirical temperature model we can calculate monthly extraterrestrial global solar radiation.

Where, Ge=9.297 kWh/m$^2$/day, Ki=0.16 for the interior region, maximum and minimum temperature of January months of the site at 2011 is 29.65℃, and 10.1℃ is taken from National Meteorological Agency (NAMA) respectively.

$$\frac{G}{Ge} = \xi(\ \Delta T)^{0.5})$$

$$G = Ge(\xi)(\ Tmax - Tmin)^{0.5}$$

$$\text{G} = 9.297(0.16)(\ 29.65 - 10.1)^{0.5}$$

G=6.563 kWh/m$^2$/day.

Monthly global solar radiation is also calculated and listed below in the table for each location. Temperature data is recorded from the National Meteorological Agency from 2011 to 2016 for six years.

Table 3. 3 Summarized average yearly distribution of Adama

| Months | Days | $\phi$(deg) | θ ($d$eg) | $\omega_a$ | Tmin (℃) | Tmax (℃) | $\xi$ | Ge | G |
|---|---|---|---|---|---|---|---|---|---|
| Jan | 31 | 8.526 | -17.78 | 87.25 | 10.1 | 29.65 | 0.16 | 9.2770 | 6.563 |
| Feb | 59 | 8.526 | -8.67 | 88.71 | 11.7 | 31.83 | 0.16 | 10.016 | 7.190 |
| March | 90 | 8.526 | 3.62 | 90.51 | 13.7 | 33.37 | 0.16 | 10.478 | 7.435 |
| April | 120 | 8.526 | 14.58 | 92.23 | 13.9 | 33.4 | 0.16 | 10.474 | 7.400 |
| May | 151 | 8.526 | 21.89 | 93.45 | 14.3 | 32.53 | 0.16 | 10.238 | 6.994 |
| Jun | 181 | 8.526 | 23.18 | 93.70 | 15.6 | 33.08 | 0.16 | 9.7680 | 6.534 |
| Jul | 212 | 8.526 | 18.17 | 92.84 | 14.2 | 30.33 | 0.16 | 10.290 | 6.612 |
| Aug | 243 | 8.526 | 8.10 | 91.20 | 15 | 28.02 | 0.16 | 10.401 | 6.004 |
| Sept | 273 | 8.526 | -3.82 | 90.60 | 14.3 | 28.67 | 0.16 | 10.103 | 6.128 |
| Oct | 304 | 8.526 | -15.05 | 87.68 | 11.8 | 29.33 | 0.16 | 9.5160 | 6.375 |
| Nov | 334 | 8.526 | -21.97 | 86.56 | 11.1 | 29.45 | 0.16 | 8.9390 | 6.127 |
| Dec | 365 | 8.526 | -23.08 | 86.30 | 10.3 | 28.45 | 0.16 | 8.8630 | 6.041 |

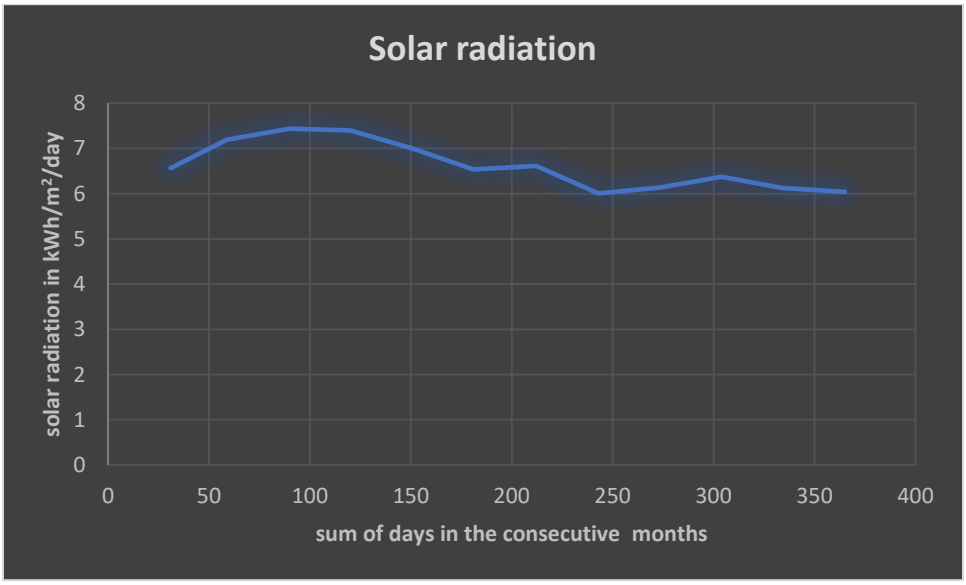


Figure 3. 3 Solar Radiation distribution throughout the year at Adama

Table 3. 4 Summarized average yearly distribution of Metehara

| Months | Days | $\phi$(deg) | Θ($d$eg) | ωa | Tmax(℃) | Tmin(℃) | $\xi$ | Ge | G |
|---|---|---|---|---|---|---|---|---|---|
| Jan | 31 | 8.9 | -17.78 | 87.13 | 34.21 | 9.42 | 0.16 | 9.319 | 7.424 |
| Feb | 59 | 8.9 | -8.67 | 88.65 | 36.60 | 15 | 0.16 | 9.995 | 7.432 |
| March | 90 | 8.9 | 3.62 | 90.54 | 36.41 | 16 | 0.16 | 10.452 | 7.555 |
| April | 120 | 8.9 | 14.58 | 92.33 | 36.30 | 15.5 | 0.16 | 10.49 | 7.655 |
| May | 151 | 8.9 | 21.89 | 93.59 | 38.58 | 18.43 | 0.16 | 10.261 | 7.369 |
| Jun | 181 | 8.9 | 23.18 | 93.86 | 38.82 | 18.29 | 0.16 | 10.170 | 7.373 |
| Jul | 212 | 8.9 | 18.17 | 92.96 | 37.72 | 18.91 | 0.16 | 10.295 | 7.144 |
| Aug | 243 | 8.9 | 8.10 | 91.26 | 35.33 | 15.81 | 0.16 | 10.396 | 7.350 |
| Sept | 273 | 8.9 | -3.82 | 89.37 | 35.12 | 17.67 | 0.16 | 10.113 | 6.759 |
| Oct | 304 | 8.9 | -15.05 | 87.57 | 35.42 | 12.53 | 0.16 | 9.4620 | 7.243 |
| Nov | 334 | 8.9 | -21.97 | 86.41 | 34.92 | 11.15 | 0.16 | 8.876 | 6.924 |
| Dec | 365 | 8.9 | -23.08 | 86.14 | 33.87 | 9.67 | 0.16 | 8.801 | 6.927 |

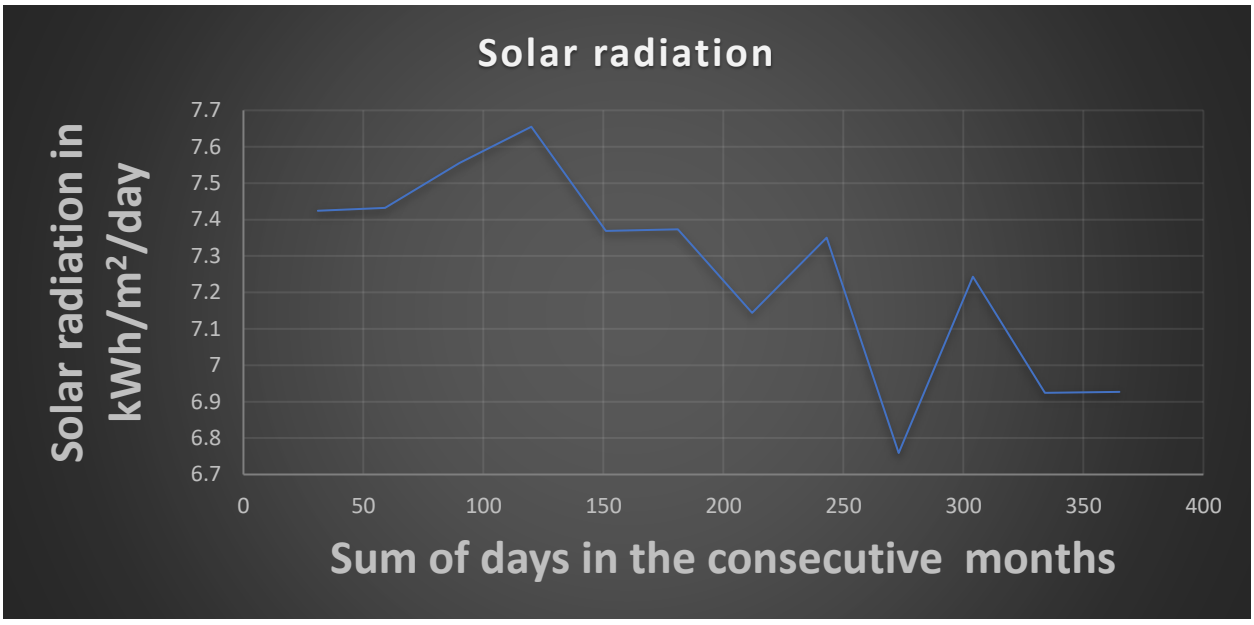


Figure 3. 4 Solar Radiation distribution throughout the year at Metehara

Table 3. 5 Summarized average yearly distribution of Awash Arba

| Months | Days | $\phi$(deg) | $\theta$($d$eg) | $\omega_a$ | Tmax(°C) | Tmin(°C) | $\xi$ | Ge | G |
|---|---|---|---|---|---|---|---|---|---|
| Jan | 31 | 11.756 | -17.78 | 86.18 | 34.48 | 15.4 | 0.16 | 8.879 | 6.205 |
| Feb | 59 | 11.756 | -8.67 | 88.18 | 36.37 | 17.5 | 0.16 | 9.785 | 6.801 |
| March | 90 | 11.756 | 3.62 | 90.75 | 36.70 | 17.75 | 0.16 | 10.423 | 7.260 |
| April | 120 | 11.756 | 14.58 | 93.10 | 37.43 | 18.75 | 0.16 | 10.60 | 7.330 |
| May | 151 | 11.756 | 21.89 | 94.79 | 38.37 | 19.43 | 0.16 | 10.48 | 7.297 |
| Jun | 181 | 11.756 | 23.18 | 95.10 | 38.85 | 17.68 | 0.16 | 10.405 | 7.660 |
| Jul | 212 | 11.756 | 18.17 | 93.91 | 38.25 | 17.55 | 0.16 | 10.468 | 7.620 |
| Aug | 243 | 11.756 | 8.10 | 91.69 | 37.28 | 17.65 | 0.16 | 10.419 | 7.386 |
| Sept | 273 | 11.756 | -3.82 | 89.20 | 37.15 | 18.63 | 0.16 | 9.966 | 6.862 |
| Oct | 304 | 11.756 | -15.05 | 86.78 | 37.31 | 18.38 | 0.16 | 9.171 | 6.384 |
| Nov | 334 | 11.756 | -21.97 | 85.19 | 36.63 | 17.37 | 0.16 | 8.538 | 5.995 |
| Dec | 365 | 11.756 | -23.08 | 84.91 | 36.30 | 17.03 | 0.16 | 8.398 | 5.898 |

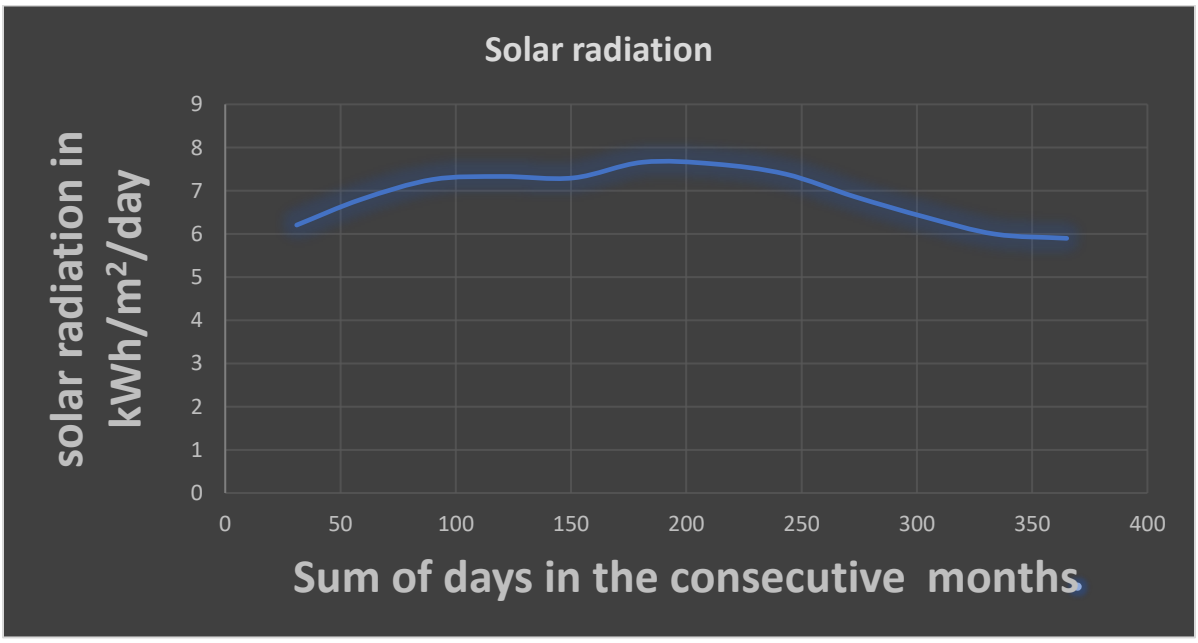


Figure 3. 5 Solar Radiation distribution throughout the year at Awash Arba

Table 3. 6 Summarized average yearly distribution of Asebe Teferi

| Months | Days | $\phi$(deg) | θ ($d$eg) | $\omega_a$ | Tmax(℃) | Tmin(℃) | $\xi$ | Ge | G |
|---|---|---|---|---|---|---|---|---|---|
| Jan | 31 | 9.08 | -17.78 | 87.06 | 28.43 | 10.62 | 0.16 | 9.286 | 6.270 |
| Feb | 59 | 9.08 | -8.67 | 88.60 | 30.12 | 12.02 | 0.16 | 9.976 | 6.790 |
| March | 90 | 9.08 | 3.62 | 90.58 | 31.15 | 13.20 | 0.16 | 10.457 | 7.088 |
| April | 120 | 9.08 | 14.58 | 92.38 | 31.10 | 13.50 | 0.16 | 10.481 | 7.035 |
| May | 151 | 9.08 | 21.89 | 93.69 | 30.22 | 14.25 | 0.16 | 10.269 | 6.566 |
| Jun | 181 | 9.08 | 23.18 | 93.93 | 30.73 | 14.72 | 0.16 | 10.179 | 6.516 |
| Jul | 212 | 9.08 | 18.17 | 93.00 | 29.88 | 14.03 | 0.16 | 10.302 | 6.562 |
| Aug | 243 | 9.08 | 8.10 | 91.30 | 29.72 | 14.03 | 0.16 | 10.393 | 6.587 |
| Sept | 273 | 9.08 | -3.82 | 89.37 | 29.78 | 14.07 | 0.16 | 10.099 | 6.404 |
| Oct | 304 | 9.08 | -15.05 | 87.52 | 29.48 | 13 | 0.16 | 9.436 | 6.130 |
| Nov | 334 | 9.08 | -21.97 | 86.30 | 29.52 | 13.17 | 0.16 | 8.849 | 5.725 |
| Dec | 365 | 9.08 | -23.08 | 86.09 | 29.42 | 12.73 | 0.16 | 8.770 | 5.732 |

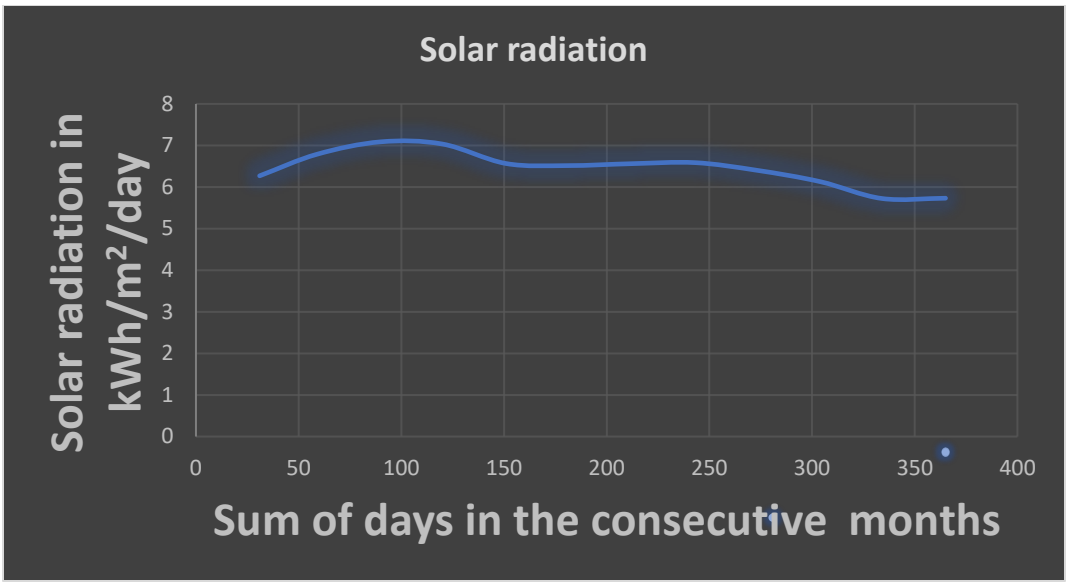


Figure 3. 6 Solar Radiation distribution throughout the year at Asebe Teferi

The accuracy of the estimated values was tested by computing the Mean Bias Error (MBE), Root Mean Square Error (RMSE), and Mean Percentage Error (MPE).

$$MBE = \frac{1}{n}\sum_{n=1}^{n}(\text{Gi, estimated} - \text{Ge, i, meas ur ed}) \quad 3.12$$

$$\text{RMSE} = [\frac{1}{n}\sum_{n=1}^{n}(\text{G i, estimated} - \text{Ge, } i\text{, meas ured})^2]^{1/2} \quad 3.13$$

$$\text{MPE} = \frac{1}{n}\sum_{n=1}^{n}\left(\left(\frac{\text{G}i,\ \text{estimated}-\text{Gi,\ measured}}{\text{Gi,\ measured}}\right) * 100\right) \quad 3.14$$

Where, G, i$^{th}$ measured is i$^{th}$ measured values of daily global solar radiation, G, $i^{th}$, calculated is i$^{th}$ calculated values of daily global solar radiation and n is the total number of observations/measurements.

Table 3. 7 The estimated and measured solar radiation for Adama

| Months | Jan | Feb | Mar | Apr | May | Jun | Jul | Aug | Sept | Oct | Nov | Dec |
|---|---|---|---|---|---|---|---|---|---|---|---|---|
| Gi, esti | 6.563 | 7.19 | 7.435 | 7.4 | 6.994 | 6.534 | 6.612 | 6.004 | 6.128 | 6.375 | 6.127 | 6.041 |
| Gi, meas | 6.49 | 7.08 | 7.21 | 7.26 | 7.11 | 6.52 | 6.58 | 6.78 | 6.88 | 6.85 | 6.49 | 6.36 |

$MBE = \frac{1}{n}\sum_{n=1}^{n}(Gi, \text{estimated} - Gi, \text{measured})$ = -0.1839

$\text{MPE} = \frac{1}{n}\sum_{n=1}^{n}\left(\left(\frac{\text{Gi, estimated}-\text{Gi, measured}}{\text{Gi, measured}}\right) * 100\right) = 2.76\%$

$\text{RMSE} = [\frac{1}{n}\sum_{n=1}^{n}(Gi, \text{estimated} - Gi, \text{measured})^2]^{1/2} = 0.3796$

Table 3. 8 The estimated and measured solar radiation for Metehara

| Months | Jan | Feb | Mar | Apr | May | Jun | Jul | Aug | Sept | Oct | Nov | Dec |
|---|---|---|---|---|---|---|---|---|---|---|---|---|
| Gi,esti | 7.424 | 7.432 | 7.555 | 7.655 | 7.369 | 7.373 | 7.144 | 7.35 | 6.76 | 7.243 | 6.924 | 6.927 |
| Gi,meas | 6.49 | 7.08 | 7.21 | 7.26 | 7.11 | 6.52 | 6.58 | 6.78 | 6.88 | 6.85 | 6.49 | 6.36 |

$MBE = \frac{1}{n}\sum_{n=1}^{n}(Gi, \text{estimated} - Gi, \text{measured})$ = 0.4622

$\text{MPE} = \frac{1}{n}\sum_{n=1}^{n}\left(\left(\frac{\text{Gi, estimated}-\text{Gi, measured}}{\text{Gi, measured}}\right) * 100\right)$ = -6.897%

$\text{RMSE} = [\frac{1}{n}\sum_{n=1}^{n}(Gi, \text{estimated} - Gi, \text{measured})^2]^{1/2} = 0.1534$

Table 3. 9 The estimated and measured solar radiation for Awash Arba

| Months | Jan | Feb | Mar | Apr | May | Jun | Jul | Aug | Sept | Oct | Nov | Dec |
|---|---|---|---|---|---|---|---|---|---|---|---|---|
| Gi,esti | 6.205 | 6.80 | 7.26 | 7.33 | 7.297 | 7.66 | 7.62 | 7.386 | 6.862 | 6.384 | 5.995 | 5.898 |
| Gi,meas | 6.65 | 7.21 | 7.36 | 7.32 | 7.17 | 6.64 | 6.63 | 6.84 | 7.07 | 7.02 | 6.61 | 6.48 |

$MBE = \frac{1}{n}\sum_{n=1}^{n}(Gi, \text{estimated} - Gi, \text{measured})$ = 0.03975

$$\text{MPE} = \frac{1}{n}\sum_{n=1}^{n}\left(\left(\frac{\text{Gi, estimated} - \text{Gi, measured}}{\text{Gi, measured}}\right) * 100\right) = 0.0833\%$$

$$\text{RMSE} = [\frac{1}{n}\sum_{n=1}^{n}(Gi, \text{estimated} - Gi, \text{measured})^2]^{1/2} = 0.3175$$

Table 3. 10 The estimated and measured solar radiation for Asebe Teferi

| Months | Jan | Feb | Mar | Apr | May | Jun | Jul | Aug | Sept | Oct | Nov | Dec |
|---|---|---|---|---|---|---|---|---|---|---|---|---|
| Gi,esti | 6.27 | 6.79 | 7.088 | 7.035 | 6.566 | 6.516 | 6.562 | 6.587 | 6.404 | 6.13 | 5.725 | 5.732 |
| Gi,meas | 6.52 | 7.07 | 7.33 | 7.30 | 7.13 | 6.46 | 6.52 | 6.76 | 6.92 | 6.94 | 6.6 | 6.33 |

$$MBE = \frac{1}{n}\sum_{n=1}^{n}(Gi, \text{estimated} - Gi, \text{measured}) = -0.3729$$

$$\text{MPE} = \frac{1}{n}\sum_{n=1}^{n}\left(\left(\frac{Gi, \text{ measured} - Gi, \text{ estimated}}{Gi, \text{ measured}}\right) * 100\right) = 5.4598$$

$$\text{RMSE} = [\frac{1}{n}\sum_{n=1}^{n}(Gi, \text{estimated} - Gi, \text{measured})^2]^{1/2} = 0.1361$$

These above results of each site show good agreement on MPE (MPE $\leq \pm 10\%$) between the estimated and measured global solar radiation by using temperature-based models. And also, MBE results from the agreement of uncertainty and value is between intervals ±5, and in the above results of RMSE value small so, used temperature-based model is good to estimate the global solar radiation and increases the confidence level of the model used.

Minimum and maximum solar radiation of location for Adama, Metehara, Awash, and Asebe Teferi are 6.041 and 7.435 kWh/m$^2$/day, 6.927, and 7.655 kWh/m$^2$/day, 5.898 and 7.66 kWh/m$^2$/day, and 5.725 and 7.088 kWh/m$^2$/day respectively.

## 3.3. Energy Calculation

Energy is one of the most promising demands which plays a major role in economic growth. There are several factors to size energy such as urbanization, modernization, and increasing human population size which leads to increase energy demand. Energy consumption increases by the rate of 1% for developed nations while 5% for developing nations.

Solar energy is considered one of the most important types of renewable energy types. The advantages of solar energy are clean, carbon-free, and availability.

Solar energy with high solar radiations, a long duration of sunshine hours, and gentle topography is the most feature for installing a solar PV system for different uses. The average daily global solar radiation at the horizontal surface of the selected site area is 6.617 kWh/$m^2$/day for Adama, 7.263 kWh/$m^2$/day for Metehara, 6.891 kWh/$m^2$/day for Awash Arba, and 6.45 kWh/$m^2$/day for Asebe Teferi [26].

According to international standards, if the average daily global solar radiation is above 3.5 kWh/$m^2$/day the use of solar modules is very economical and affordable. In many parts of the country like Adama, Metehara, Awash Arba, and Asebe Teferi, solar radiation energy is higher than the international standards, and in some places, measured solar radiation is higher than 7 to 8 kWh/$m^2$/day. The calculation of the solar energy is based on the location and average monthly of the yearly global solar radiation. The solar energy calculation for different geographical latitudes and inclination angles will be calculated in the following ways. In the design plan of grid-connected PV system the total daily, monthly and annual consumption of the trainloads should be considered. The daily and monthly energy consumption loads of trains should be known and taken from ERC or Ethiopian Electric Utility, but the daily and monthly energy consumption of the train is based on the assumption. Loads of railway are train and some auxiliary loads like lighting and traffic signals in the section end. Then, from the technical proposal of the Ethiopian Railway Corporation, the maximum load for an electric train car is 815.4 kW to accommodate this load the generated power from the renewable resource should be greater than the loads which mean for this thesis is 1 MW will be considered.

## 3.4. The Average Daily Solar Radiation Intensity

The site in Ethiopia like Adama, Metehara, Awash Arba and Asebe Teferi in the train route of Ethio-Djibouti railway has a high solar energy potential, where the monthly average global solar radiation intensity is 6.617 kWh/m2/day for Adama, 7.263 kWh/$m^2$/day for Metehara, 6.891 kWh/$m^2$/day for Awash Arba and 6.45 kWh/$m^2$/day for Asebe Teferi.

## 3.5. Installation of the PV system

The selected PV system for the above site is the monocrystalline type of panel which is used with having the specification below. Monocrystalline panel which is used in work has the following characteristics: cost-effective in the long term, lower installation costs, space use is efficient, non-hazardous to the environment, cleans themselves each time, performs better in the low light

conditions when compared to polycrystalline PV modules. The maximum amount of light to reach the silicon cells and along with the anti-reflective coating and great in the heat resistance are some of the characteristics of the monocrystalline PV module. The selected PV module having 345 Watts of the specification is perfect for grid-connected solar systems. The PV panel guarantees 25 years to produce 80% of the rated output throughout the lifetime of the project.

## 3.6. System Sizing

System sizing is the process of evaluating the adequate voltage and current ratings for each component of the photovoltaic system to meet the electric demand at the train loads and at the same time calculating the total price of the entire system from the design phase to full system functionality including labor cost.

Table 3. 11 Specifications of PV module

| Electrical Data for model NC-345M-72 | |
|---|---|
| Maximum Power | 345 W |
| Maximum Power Voltage | 1000 V |
| Open circuit voltage, $V_{oc}$ | 46.9 V DC |
| Short Circuit Current, Isc | 9.29 A |
| Maximum power voltage | 39.1 V |
| Maximum power current | 8.84 A |
| Cells per module | 72 |
| Cell type | Monocrystalline |
| Dimensions | 1960mm L x 992mm W x 40mm'' H |
| Maximum Power Tolerance | -0% to +3% |
| Maximum wind resistance | 60 m/s |

### 3.6.1. Sizing of the PV system

Before sizing of PV array, the total energy in watt-hour, average sunshine hour per day, minimum and maximum temperature, the DC voltage, and AC output voltage of inverter should be determined and once these factors are available, the process of sizing can be started.

To avoid under-sizing of the system the total average energy demand per day can be divided by overall efficiencies of the system components to obtain the daily energy requirement from the solar array:

Then,

$$E_{dre} = \frac{Et}{\eta overall} \quad 3.15$$

where, $E_{dre}$ is a daily energy requirement from the solar array, $E_t$ is daily average energy consumption and ηoverall is a product or overall efficiencies of the system components.

The peak power of the PV generator or PV array is obtained by the following formula.

$$P_{pv} = \frac{E_{dre}}{P_{sh}} \quad 3.16$$

where, $P_{pv}$ is the peak power of PV array, $P_{sh}$ is the minimum peak hour of sun hours per day.

The total DC needed can be calculated by the following formula.

$$I_{dc} = \frac{P_{pv}}{V_{dc}} \quad 3.17$$

where, $I_{dc}$ is total DC current and $V_{dc}$ is the DC voltage of the PV array or system.

### 3.6.2. Sizing of Inverter

In this system, the inverter is used to convert direct current (DC) into alternating current (AC) and feeds into load and the electrical grid. The inverter must be synchronized or in phase with that of the grid and used to limit its voltage not higher than that of the grid voltage.

In the inverter sizing the one we have to consider is the capability of handling the maximum expected power of AC loads. The input voltage of the inverter has to be matched with the boost converter output. The output value inverter is 1500/1600 V and should fulfill the specifications of the 25 kV grid.

To size the inverter suitable to the PV system, the main parameters should be determined.

The parameters are as follows: the inverter output voltage should fulfill the specification of the electric grid specified with a rated voltage of the trainload is around 1500/1600 V AC±5%. The nominal power of the inverter must be greater than the total power of the load of 815.4 kW and which is equal to 1MW. The maximum inverter output current is found by dividing the total load power by the system voltage. The value will be taken from the datasheet of the manufacturer. Inverter to load current is equal to total load power divided by the system voltage which is 1600 V. The efficiencies of the inverter lie between 95%-98%.

And also, inverter sizing depends on the array or module peak power. The array peak power is calculated as follows:

Array peak power is equal to many modules in the array times the rated maximum power ($P_{mp}$) of selected modules at STC.

The selected PV module has an output power of 345 W then, array peak power having 11 modules in one array is equal to (345*2904=1.002MW). To facilitate the efficient design of PV systems, the inverter nominal power output cannot be less than 75% of the peak array power and it should not be outside the inverter manufactures maximum allowable array size specifications [27].

Then, in the sizing of the inverter first, the value of power of the load or energy consumption at a time in the sections should be known. And also, the selected inverter should be able to handle 815.4 kW amount of power at a time. In addition to these requirements, a voltage operating point has to add. If the solar array voltage is outside this operating window then, either the inverter will not operate or the output power of the system will be greatly reduced [28].

The selection of the inverter for the installation will depend on the energy output of the array, the matching of the allowable inverter string configurations with the size of the array kW or MW. These inverters are used to utilized and convert the high-level DC voltage to the AC Voltage to supply the loads. There are four basic solar PV system inverter configurations.

#### 3.6.2.1. Single Stage Centralized Inverter

Photovoltaic modules or array are connected in series to form a photovoltaic string to reach a higher voltage.

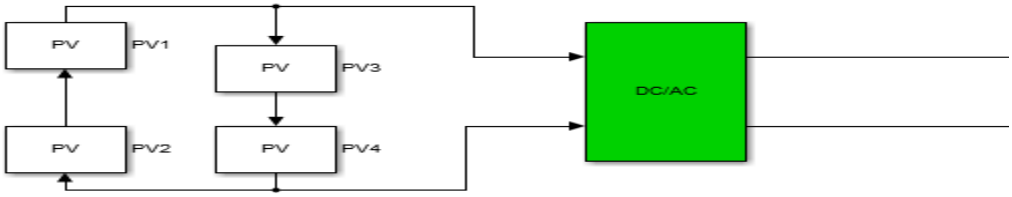


Figure 3. 7 Single Stage Centralized Inverter

#### 3.6.2.2. Single Stage String Inverter

In this configuration, each PV string can have its maximum power point and it is best if there any partial shading or panel mismatch. Each string inverter is supposed to handle its own maximum power point tracking and power conversion control. This one best performance due to the inverter applied to each PV string but, the string inverter configuration increases the total cost of installation.

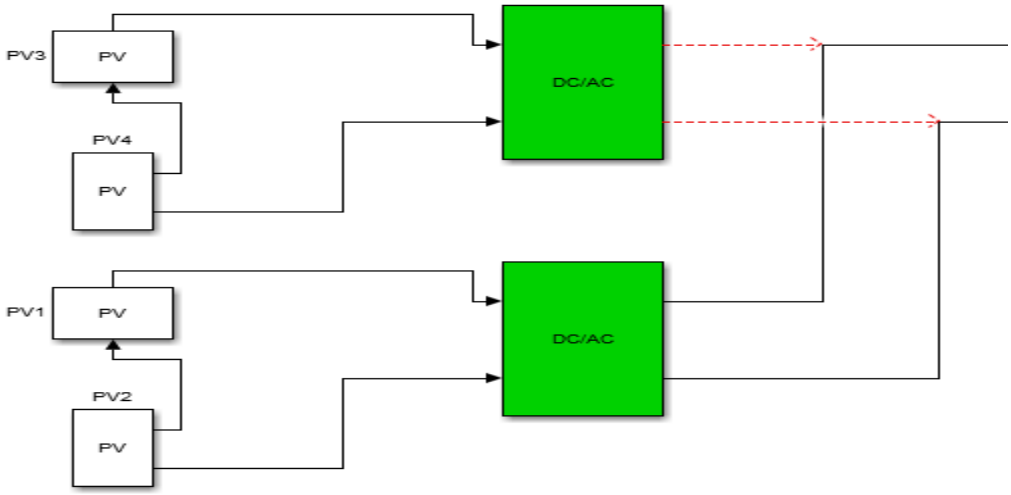


Figure 3. 8 Single Stage String Inverter

#### 3.6.2.3. Two-stage String Inverter

This configuration is popular due to improved energy harvesting capability, modularity, and design flexibility. Each photovoltaic string contains less solar panels or array which increases the system robustness and for this thesis, such kind of design is considered. The first stage is to increase or amplify low DC voltage generated by solar panels to a higher-level DC bus. The converter should also handle the maximum power point tracking.

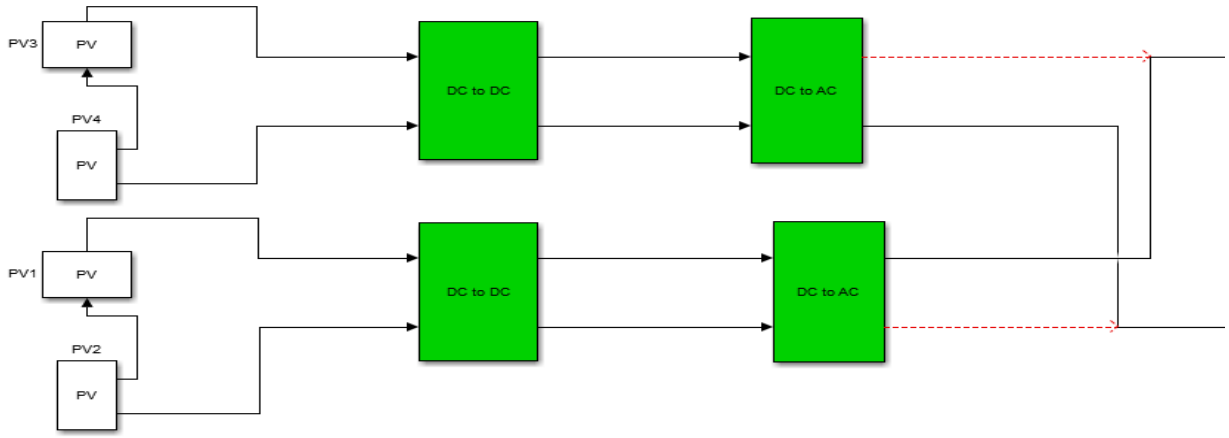


Figure 3. 9 Two-Stage String Inverter

#### 3.6.2.4. Two-Stage Centralized Inverter

The first task in this inverter is the amplification of the DC voltage by using DC to DC converter. The second task is the output of the converter is supplied to the centralized DC to AC inverter. This type of configuration may reduce the cost of an inverter however, the centralized inverter may be larger and there is no such kind of inverter availability in the market for single-phase higher power.

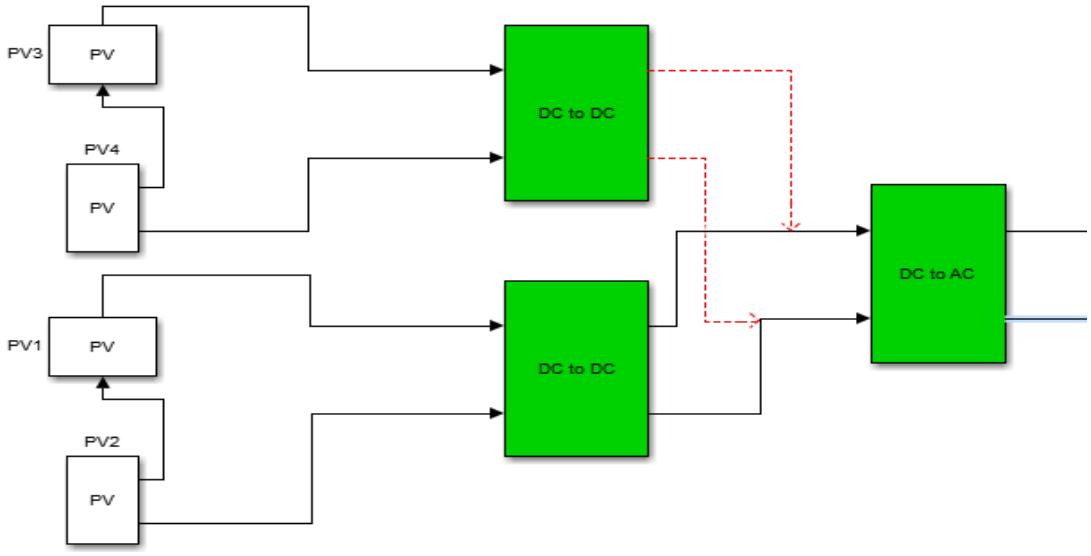


Figure 3. 10 Two-Stage Centralized Inverter

Specifications of 100 KVA Inverter

Table 3. 12 Inverter specifications

| | |
|---|---|
| Model Number | NB220-100KDZ |
| Power | 80 kW |
| Nominal DC voltage | 220 V |
| Nominal DC current | 455 A |
| Maximum AC power | 80 kW |
| Output AC voltage range | 95.7-276 V |
| Frequency | 50, 60 Hz |
| Power factor | 0.8 |
| THD | <3 % |
| Number of feed-in phases | 1 |
| Maximum efficiency | 98% (EURO 0.108/Wp) |

The selected inverter for the grid-connected PV system specification currently higher power of 100 kVA inverter is available in the market so, 10 two-stage string inverters can be used to accommodate loads of 1MW[29],[26].

## 3.7. Energy production Estimation

The system energy output over a whole year is known as the systems energy yield. The average energy yield for this thesis work is determined as follows:

$$Esyst = PVarry_{STC} * \eta * \mathrm{G} * \mathrm{A} \qquad 3.18$$

Where: PVarry_STC is a photovoltaic array at standard test conditions, average daily global solar radiation in the horizontal surface, and η is the overall efficiency of the PV system.

It is recommended that the maximum voltage drop or losses between PV arrays and the inverter is 3% and the voltage drop between the inverter and grid is 1%.

AC energy output of the PV array is dependent on the above factors, orientation (Azimuth), and tilt. PV orientation is true north (Azimuth is zero) with an inclination equal to the latitude angle.

Overall efficiency is dependent on derating factors like manufacturing tolerance, mismatch and cable loss, dust loss, DC to AC loss, and temperature loss. According to the international agreement that the loss is figured as follows in Table 3.13 given below.

De rating factor analysis is used to determine the performance of the overall single-phase grid-connected photovoltaic system.

Let the average ambient temperatures of the site is 30 Degree Celsius, tolerance is +/-5% and derating due to temperature is +/-5% due to the region which is interior. At the beginning of this thesis 345W of Monocrystalline PV panels is selected then, the output can be determined as follows:

$$\text{Pde} = 0.95 * 0.95 * 0.865 * 345\text{W} = 269.3\ \text{W}$$

where, $P_{der}$ is derated Output power.

### 3.7.1. Energy Produced from Photovoltaic Array

The actual DC energy ($E_{dc}$) from the solar array is equal to multiple of the derated output power ($P_{der}$) of the module, many solar panels, solar Irradiation of the site (G), and area of the modules (A).

Which is:

$$E_{dc} = P_{der} * No.panel * G * A \qquad 3.19$$

If we considered a total number of the modules for this thesis 2904 modules and the average solar radiation of the site (Awash Arba) G is equal to 6.891 kWh/$m^2$/day.

Where: $P_{der}$ is equal to 269.3W, No. panel is equal to 2904, and G is equal to 6.891 kWh/$m^2$/day for Awash Arba.

$$E_{dc} = 269.3\text{W}\frac{* 2904\ * 6.891\frac{\text{kWh}}{\text{m2}}}{\text{day}} * 1.944\text{m2} = 10476385.624\ \text{WH}$$

By considering all losses formulation is seen in the table below.

Table 3. 13 Output power by considering the losses of the system

| No. | Efficiency | DC energy due to loss |
|---|---|---|
| 1 | $\eta_{DC,\ system} = 0.97$ | 10162094.06 Wh |
| 2 | $\eta_{inv} = 0.98$ | 9958852.17 Wh |
| 3 | $\eta_{AC,\ system} = 0.99$ | 9859263.65 Wh |

The average daily AC energy delivered from the array to the grid equal to 9859.264 kWh. Therefore, over a typical year of 365 days then the energy yield of the solar array is:

$$E_{ac,\ year} = 365 * 9859.264\ \text{kWh} = 3598.632\ \text{MWh}$$

## 3.8. Performance Ratio for this Grid-Connected System

The performance ratio (PR) is used to access the installation quality of the PV system. Specifically, in this thesis work, Monocrystalline PV modules were considered but, performance ratio is used to compare different types and sizes of PV modules and also used to analyze the system losses. Performance ratio PR of actual yearly energy yield from the system E sys and the ideal energy output of the array E ideal.

The photovoltaic arrays ideal energy yield E ideal can be determined as follows:

$$E_{ideal} = \text{P arry\_STC} * \text{G} * \text{A} \qquad 3.20$$

$$E_{ideal,\ daily} = 345 * 2904 * \frac{6.891\text{kWh}}{\text{m2}} * 1.944\text{m2} = 13421288.67\text{kWh}$$

Then, throughout the year ideal energy E $_{\text{ideal}}$ is equal to 365 times $E_{ideal,\ daily}$ which is equal to 4898.77 MWh.

If the performance ratio is considered shading loss with negligible value then, for this system shading is eliminated for estimation of real energy yield.

Therefore, the performance ratio is determined as follows:

$PR = \frac{Esys}{Eideal} = \frac{3598.632\ \text{MWh}}{4898.77\ \text{MWh}} = 0.735$. Then, the loss is 26.5%.

## 3.9. Modules Mounting and Spacing Geometry

Solar modules perform best when the panels are mounted perpendicular to the sun's rays. Mounting solar panels are analyzed by facing the effectiveness of mounting either south, southeast, north, and soon but, all modules facing due south will meet the largest power of any other arrangement. In module mounting in the same way tilt angles should be considered. The sun position varies due to seasonal variation so, adjustment my needed to track more power from the sun. As we know the rule of thumb says that latitude plus 15 degrees in winter season and latitude minus 15 degrees. Ethiopia is located near to equator which means the days and nights is almost equal in all season so, the tilt angle may not require to be adjusted [30].

The spacing of the photovoltaic module depends on the length of the modules the tilt angle of 15 degrees and the latitude of the site for Awash Arba is 8.99 degrees. While the shadows of the site area are to be considered as undesirable.

The geometrical relationship between the angles and modules is shown below [31].

The minimum module spacing between rows is formulated as follows:

$$X = \frac{L*\sin ß}{\tan \phi} \qquad 3.21$$

Where: $X$ is module spacing or Row space,

L =1.996m is the length of the module

ß =15 degree is tilt angle and

ϕ =8.9917 degree is the latitude of the site

Sizing a tilted array

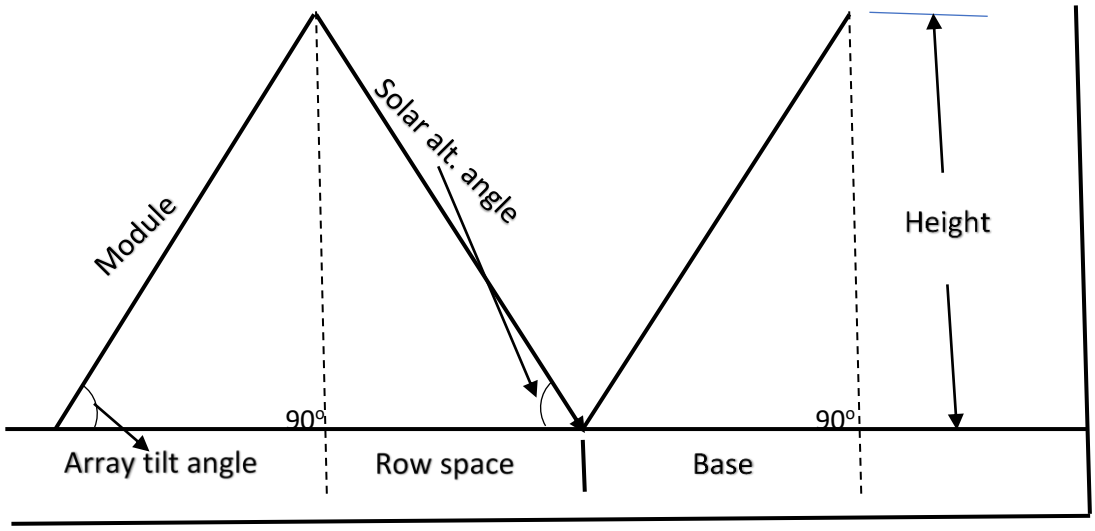


Figure 3. 11 Spacing Geometry of PV Module

By substituting the value, the module spacing can be determined as follows:

$$x = \frac{\text{L sin ß}}{\tan\phi} = \frac{1.96 \sin 15}{\tan 8.9917} = 3.206\text{m}$$

## 3.10. Photovoltaic Cell modeling

The ideal photovoltaic cell modeling consists of a real diode in parallel with an ideal current source. The ideal current source is used to delivers current from the material cell in the form of solar flux.

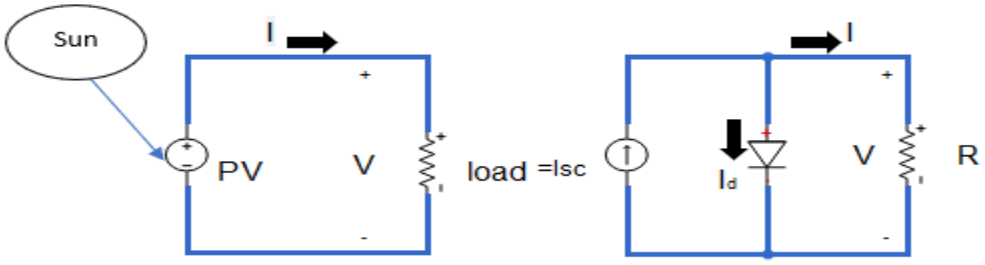


Figure 3. 12 Photovoltaic Cell

The practical photovoltaic modeling in this research work is modeled as one diode model. Photovoltaic system output $i_{ds}$ dependent on temperature and solar radiation. The circuit model is explained below: the followings are the variables of photovoltaic cell modeling temperature dependence on the reserved saturation current Is, the temperature dependence of the photocurrent $I_{ph}$, shunt resistance $R_{sh}$ in parallel with the diode, and series resistance $R_s$ which is internal losses due to the current flow.

The circuit is as follows:

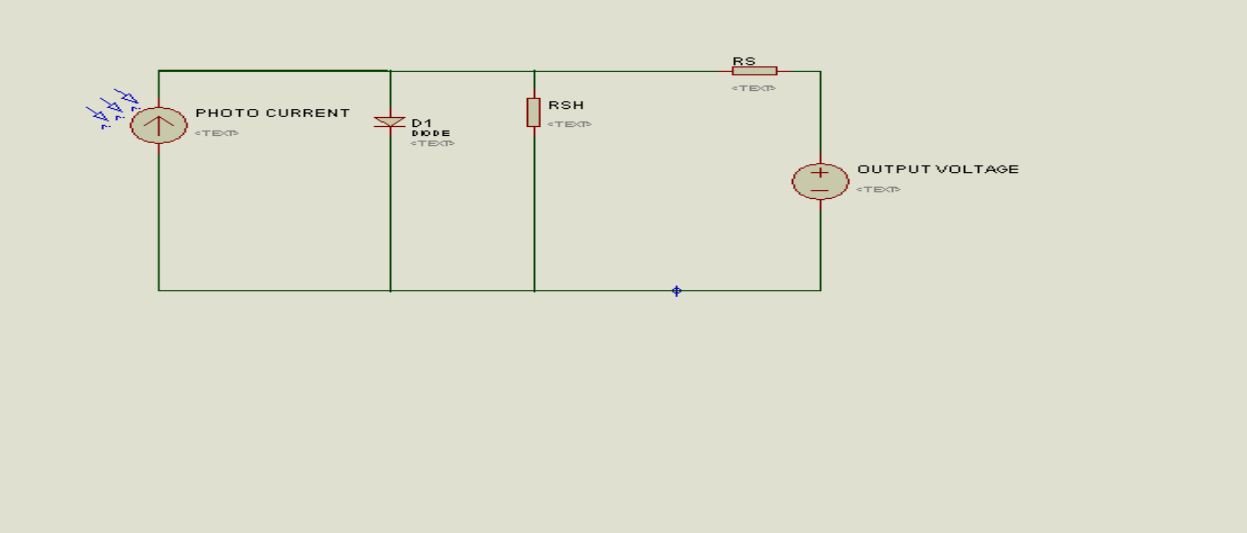


Figure 3. 13 One diode modeling of PV modules

The load current at $R_s$ (series resistor) is given by the KCL:

$$I = \left(I_{ph} * N_p\right) - I_d - I_{sh} \qquad 3.22$$

Where: $I_{ph}$ is photocurrent, $I_d$ is diode current, $I_{sh}$ is shunted current, and Np is many cells connected in parallel.

Then, the photocurrent is calculated as follows:

$$I_{ph} = K_i(I_{sc} + K_i(\mathrm{T} - T_{ref})) \qquad 3.23$$

Where: $K_i$ is the solar irradiance ratio.

The diode current is given by the exponential equation:

$$I_d = [e^{\frac{V+IRs}{nVtCNs}} - 1] * [I_s * N_p] \qquad 3.24$$

The current flowing through parallel resistance is given as follows:

$$I_{sh} = \frac{V+IRs}{Rsh} \quad 3.25$$

The saturation current is given as follows:

$$I_s = I_{rs}\left(\frac{Top}{Tref}\right) e^{\left[\frac{qEg}{nK}\left(\frac{1}{Top} - \frac{1}{Tref}\right)\right]} \quad 3.26$$

The reverse saturation current is given as follows:

$$I_{rs} = \frac{Isc}{\left[e^{\left(\frac{Vocq}{KCTopn}\right)} - 1\right]} \quad 3.27$$

Where: K is the Boltzmann constant which is (1.38x $10^{-23}$ J/K), q is the electric charge (1.602x$10^{-19}$ c), T is the cell temperature (K) which is given by cell manufacturer, n is the diode ideality factor, $R_s$ is the series resistance, $R_{sh}$ is the shunt resistance, C is shape factor, $K_i$ is the solar irradiance, $E_g$ is the bandgap energy of the cell (1.12Ev), Ns is the number of series-connected cells, $N_p$ is the number of the cell which is connected in parallel, $T_{op}$ is the cell operating temperature (given by the cell manufacturer), $T_{ref}$ is the cell temperature at 25 deg. Celsius, $I_s$ is diode reversed saturation current, $I_{rs}$ is diode reversed saturation current at operating temperature, $I_{sc}$ is the short circuit current(given by manufacturer ), $V_{oc}$ is the open voltage (given by manufacturer ) [32].

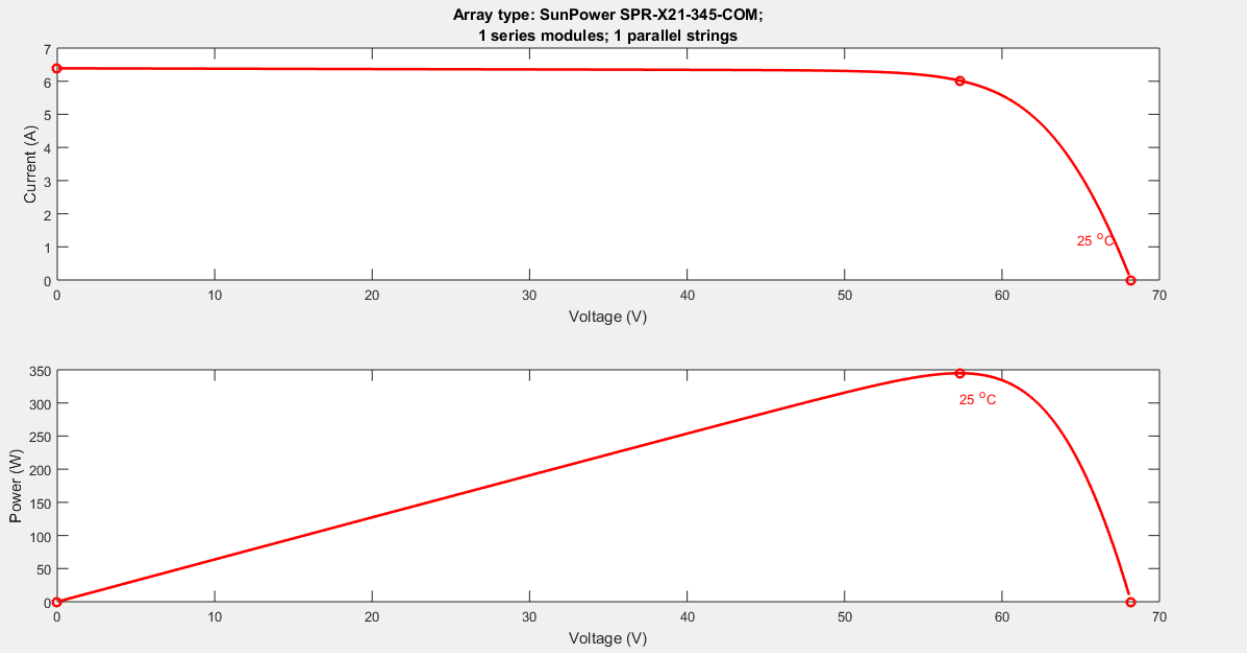


Figure 3. 14 Module I-V and P-V characteristics

## 3.11. Boost Converter Modeling

The boost converter is used to step-up DC voltage due to a drawback of that PV systems in their low efficiency. The efficiency of a solar cell is around 8 to 15%. Solar panels are capable to convert 30 to 40% of incoming solar radiation into electrical power so, MPPT is used to increase the efficiency of the solar system. The boost converter circuit mainly consists of an inductor, capacitor, resistor, and the control switch. The components are connected with source voltage to step up the output voltage.

The maximum power point tracking method for this study is the perturbed and observe method. This type of MPPT is failed to track power under fast varying temperature conditions. And very popular and simple than any other method. In the above-selected site, it is suitable to use the P & O methods of the MPPT algorithm. MPPT produces the duty cycle which is dependent on PV modules voltage and Power.

The average output voltage can be calculated by using the formula given below:

$$V_{out} = \frac{V_{in}}{1-\lambda} \qquad 3.28$$

Where: $V_{out}$ is the output voltage, $V_{in}$ is source voltage and λ is the duty cycle.

In the switching of the control switch there is ON time (ton) and OFF time (toff) then, the sum of two times is period (T) to complete the full cycle.

$$T = ton + toff \quad 3.29$$

From input to output power principles, that input power is equal to output power.

$$V_{pv} * ton = (Vout - V_{pv}) * toff \quad 3.30$$

Then, the duty cycle is equal to λ.

$$\lambda = \frac{ton}{T} \quad 3.31$$

Then, by rearranging all the above equation:

$$V_{out} = \frac{Vin}{1-\lambda} \quad 3.32$$

Ideally, the output power of the converter is equal to an input power yields.

$$Pout = Pin \quad 3.33$$

Which means,

$$Vout * Iout = Vin * Iin \quad 3.34$$

To get the desired value we have to select those boost converter components properly.
The inductor value of the boost converter is selected and determined by using the following formula:

$$L = \frac{Vin}{Fsw * \Delta Il} \quad 3.35$$

Where:

$F_{sw}$ is switching frequency and ΔIL is the input ripple current.

The current ripple factor is the ratio between input current ripple and output current. For good selection inductor CRF should bound within 30%.

$$\frac{\Delta Il}{Io} = 0.3 \quad (3.36)$$

Capacitor value can be selected by using the following formula:

$$C = \frac{Iout}{Fsw * \Delta Vo * D} \quad (3.37)$$

Where: ΔVo is the output voltage ripple which is usually considered as 5% of the output voltage which yields.

$$\frac{\Delta Vo}{Vo} = 5\% \quad (3.38)$$

Once the boost converter components parameters are selected and MPPT is considered to enhance the output power of the PV array.

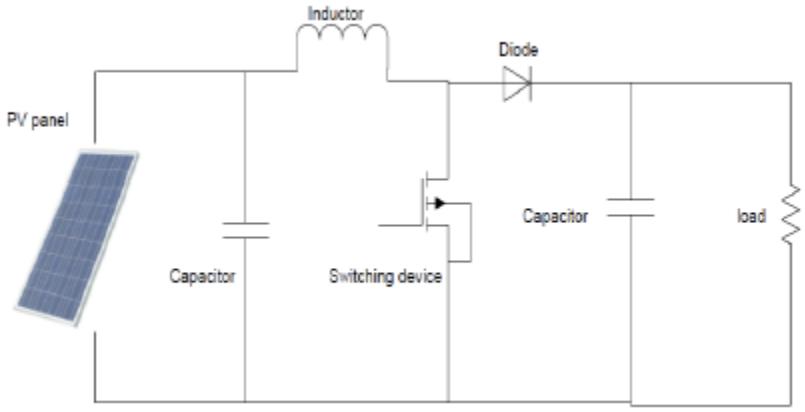


Figure 3. 15 A Boost Converter

## 3.12. Filter Design

The LCL filter is used to convert square waves into the sinusoidal wave to supply stable power quality levels. The type of filter used for this thesis work is a low pass LCL filter. In addition to

the above use LCL filter gives advantages of better decoupling between the filter and grid impedance and lower ripple current stress across the grid inductor [33]. It is also capable of limiting current inrush problems.

$$F_{res} \approx \frac{1}{2\pi} * \frac{\sqrt{L_i + L_g}}{\sqrt{L_i * L_g * Cf}} \quad 3.39$$

To avoid resonance, the resonance frequency should be:

$$10 * F_n \leq F_{res} \geq 0.5 \quad 3.40$$

$$L_i \approx \frac{E_n}{ir * F_{sw} * 2\sqrt{6}} \quad 3.41$$

$$\text{Lg} \approx \frac{L_i}{2} \quad 3.42$$

The capacitor in the LCL filter is used to avoid a low power factor and the reactive power will be caused by this capacitor. This capacitor should be less than 5% of rated active Power.

$$C_f < 0.05 * [\frac{P_n}{3 * 2\pi * {E_n}^2 * F_n}] \quad 3.43$$

Where: $P_n$ is the active power of the system, $\Delta I_{max}$ is the peak value of harmonic current, $E_n$ is the RMS value of grid voltage and $F_n$ is grid frequency (50HZ).


Figure 3. 16 LCL filter

Depending upon the above design considerations and matlab code the value of LCL parameters is $L_i$= 0.0025H, Cf = 0.25465μF and Lg = 0.0012H .

# CHAPTER FOUR

## 4. Economic Analysis of Grid-Connected Photovoltaic System

In this chapter, the cost analysis and payback of the project is analyzed by calculating the cost of generated energy from the photovoltaic system to that of utility power cost over in the year.

Estimating the cost of produced 1 kWh from the photovoltaic system depends on the lifetime cost plus the cost of income from capital investment paid in a series of regular payments in ETB or USD per kWh. A lifetime cost methodology is a useful tool to conduct a financial analysis of large-scale photovoltaic power systems. It is reasonable to use a life-cycle cost approach, particularly when we deal with renewable technologies of high initial capital costs. Costs of electric generation from photovoltaic can be broken down into the following categories: capital costs, operation and maintenance costs, replacement costs, and salvage cost. Salvage cost is the cost of destruction after the end of the project lifetime. We can assume that salvage cost after 25 years of life cycle time is negligible for this thesis work.

To estimate the project cost, the project lifetime should be known. Project lifetime depends on the PV module warranty period, which is 25 years.

Another method to estimate the project lifetime cost is fixed charges plus variable charges. Fixed charges are the cost of upfront costs, which are aggregate costs of the system components required to initiate the project and variable charges include operation and maintenance costs and cost of replacement while for fixed-tilt system and the operation and maintenance charges are assumed to be negligible. Then, variable charges are the cost of component replacement during the life period. The lifetime cost of the photovoltaic system is determined by using PV modules cost the plus cost of balance of the system. PV modules' price is based on the local or international market. Currently, PV module price is dramatically decreased from time to time and cost is around $1.018 per peak watt or 28.4 ETB per peak watt. The balance of system cost (BOS) refers to all components of a photovoltaic system other than the solar panel. The balance of the system comprises wires, switches, mounting system (supporting the panels), one or many solar inverters, converters, junction boxes with fuses and relays, power conditioners, installation, racking, labor, site preparation, and metering system. In some scholars view the balance of system or structure cost is approximately 20% of the total PV system components cost which is widely assumed overall

globe. In another way, the average cost of balance of system and installation for photovoltaic systems is in the range of $1.6 to $1.85 which is around 44.64 ETB to 51.615 ETB per peak watt [34].

The balance of system cost estimation is selected due to most of the components specification is not available in the local market so, according to the international report of cost analyzing the lifetime cost is the sum of PV module cost and cost of balance of the system. PV module is available in different sizes and types where the size of the solar panel is characterized by their peak watt at standard STC. The price of peak watt is almost the same for both monocrystalline and polycrystalline, but the installation cost will differ depending on the installed PV area. PV module preferred for this thesis is previously selected and which is monocrystalline 345W due to characteristics of fewer drops at high temperature and most widely available in the market when compared to polycrystalline.

## 4.1. Cost of PV module

The cost of the PV module is equal to the number of PV module times peak watt of PV module times cost per peak watt.

$$\text{PV module Cost} = \text{N} * \text{wattage} * \text{cost per watt} \qquad 4.1$$

Where: N is the number of solar panels, wattage is equal to the selected value which is 345 W, and cost per watt is equal to 28.504 ETB.

To generate sufficient power to run trainload at a time for Ethio-Djibouti we need more than or equal to 815.4KW power, but for this thesis, if we consider 1MW power. To generate 1MW power from the PV system we need 2904 solar panels of 345 wattages.

Costs of Elements

Table 4. 1 Cost of the components and systems

| Components | Quantity | Price in ETB |
|---|---|---|
| PV module | 2904 | 28,459,200 |
| BOS | All system cost except the panel | 44,723,923.2 |
| Total | | 73,183,123.2 |

According to a technical proposal of Ethiopian Railway Corporation number of trips per year for both Box and YZ25G of electric type trains is 275 and 550 per year respectively so, we have a minimum of three and a maximum of four trips per day from Sebeta to Awash and if we let 2 hours of operating time from Sebeta to Awash and Vic versa. Then, we can determine the per day energy consumption of the trains by multiplying power, operating time, and the number of trips per day or annually. As we know from the technical proposal of ERC power of the load is 815.4 kW then, to get the annual energy consumption of the load by multiplying power, operating time, and numbers of trips.

$$A' = P * t * N' \qquad 4.2$$

Where: $A'$ is annual energy consumption, P is power, t is operating time and $N'$ is total annual numbers of trips.

Then, based on equation (4.2):

$$A' = 815.4\ kW * 2\ Hr * 825 = 1{,}345{,}410\ kWH$$

Again, the daily energy consumption of the trainloads can be calculated by dividing annual energy consumption by the number of days in one year.

$$\text{daily energy cons} = \frac{A'}{365} = \frac{1{,}345{,}410\ kWh}{365} = 3686.05\ kWh$$

According to the Ethiopian Electric Corporation price of 1kWh is equal to 1.75 ETB.

Then, the annual cost of energy consumption is multiple of annual energy consumption and price per kWh.

$$\text{Cost of annual energy consumption} = 1{,}345{,}410 \text{ kWh} * 1.75 \text{ ETB} = 2{,}354{,}467.5 \text{ ETB}$$

Energy harassed from a solar photovoltaic system is also calculated as follows:

$$\mathrm{E} = \mathrm{A} * \mathrm{G} * \eta \text{ overall} * \mathrm{N} \qquad 4.3$$

Where: η overall is the overall efficiency of a grid-connected PV system, G is solar radiation of the site, A is an area of PV module and N is a number of PV modules.

$$E = 1.94\, m^2 * 6.891 \frac{kWh}{m^2} * 0.735 * 2904 = 28{,}534.35\, kWh$$

Then, total annual energy, $E_{tot}$ harassed from a solar photovoltaic system is equal to daily times 365 days.

$$Etot = E * 365\, days$$

$$Etot = 28534.35\, kWh * 365\, days = 10{,}415{,}036.48\, kWh$$

If we assume the price of energy generated from the photovoltaic system is the same as that of Ethiopian Electric Corporation which is 1.75 ETB.

$$\text{Annual benefi} = \text{cost of annual revenue after PV installation} - \text{costs of the annual bill before PV installation}$$

$$\text{Annual benefi} = 18{,}226{,}313.84 \text{ ETB} - 2{,}354{,}467.5 \text{ ETB} = 15{,}871{,}846.34 \text{ ETB}$$

Then, in order to calculate the payback of the project we have to use the lifetime cost divided by profit. Payback is defined as the financial return of the initial project cost after the project comes into operation.

$$\text{payback} = \frac{Initial\ investment}{profit} \qquad 4.4$$

Where: Initial investment is equal to 73,183,123.2 ETB and profit is equal to 15,871,846.34 ETB.

$$\text{Then,} \qquad \text{payback} = \frac{73{,}183{,}123.2 \text{ ETB}}{15{,}871{,}846.34 \text{ ETB}} = 4.61\ years \approx 5\ years$$

As we have seen from the analysis the initial project cost is high and payback is approximately 5 years only the then, the project is feasible[26].

## 4.2. Grid-Connected PV System Tariffs and Carbon Dioxide Emission Comparisons

Electricity delivered to the grid from the PV system composted in several ways such as net metering and feed-in tariff while in this research work net metering methods of the tariff are mainly considered.

A solar PV system generates electricity from sunlight will be used for home use and commercial building supply for business. Then, this reduces the cost of the electricity amount needed from the utility. This means that in net metering if the produced electricity is more than our demand at any given time and meter backward the power to supply grid. The utility keeps track of how much electricity will supply to the grid as well as how much purchased and the charged or billed only for our net electricity consumption via the net metering method. At the end of any billing period, if overall electricity production exceeds consumption will be indicated by negative value meter reading. The billing credit is applied to the next bill period in the net metering method.

The carbon dioxide emissions can be compared power generating from conventional power generation. Which is well know that generating power from conventional power generation there are carbon diode emissions. According to the European Photovoltaic Industry Association (EPIA), it has assumed that grid-connected PV installations will save on average of 0.6 Kg of carbon dioxide emissions equivalent per kilowatt-hour. Throughout the life cycle of the PV system emissions will be between 12g to 25g of carbon dioxide emissions equivalent to kWh. If the energy produced from the solar system throughout the life cycle of the project is equal to 208,300,729.6 kWh.

Which means:

The energy produced throughout the lifetime of the project=E*tot* *25*80%=208,300,729.6 kWh

Then, the overall carbon dioxide emissions reduction in the life cycle of the PV system is about 124,980.44 tons of carbon dioxide. So, there is no doubt that a PV system can be an effective tool to replace the conventional power generation and which is used to fight against climate change.

# CHAPTER FIVE

## 5. Control Strategies of Boost Converter and Inverter Control

Control strategies are the most important in the case of producing energy from solar PV systems in order to get output energy with less or free of harmonics. In this research work, the grid-connected solar system consists of a PV array, DC to DC converter, Inverter, and grid voltage. To control harmonics and maximize the efficiency of the system we have to use the control system and synchronization of PV array system output with the grid system is crucial.

In this thesis work, there are two kinds of control strategies used to control the whole single-phase grid-connected PV system.

The MPPT controller for DC to DC converter and inverter controller in general.

MPPT controller is used to improve the efficiency of the solar panel by adjusting source impedance to load impedance so, MPPT is equivalent to the problem of impedance matching. The output voltage is dependent on the duty cycle which means MPPT is used to determine the duty cycle to obtain the maximum output voltage and if the output voltage increase simultaneously power increases. There are several MPPT methods exists in order to maximize the output power. Those are incremental conductance method, voltage based peak power tracking method, current based peak power tracking method, perturb & observation method, and soon. Among those perturb & observation (P & O) method is used in this thesis research study. P & O method is most commonly used due to simple implementation, takes less time to track the maximum power, and economical.

### 5.1. P & O Algorithm

As the name indicates that the P & O algorithm the PV array voltage or current is perturbed by a small increment and at the resulting change in power is observed and comparing the output power with that of the previous perturbation cycle. If the change in power ($\Delta P/\Delta V>0$) is positive, the voltage is adjusted by the same increment, and the PV array operating point moves in that direction. This will continue until the change in power ($\Delta P/\Delta V<0$) is negative, at which the PV array operating point moves in the reverse direction, and the perturbation cycle continues in the same way.

Steps of P & O algorithm techniques.

i. Read the value of current and voltage from the solar PV array.
ii. Power is calculated from the measured voltage and current.
iii. The value of the voltage and power the $i^{th}$ instant is stored.
iv. The next values $(i+1)^{th}$ instant are measured again and power is calculated from the measured values.
v. The power and voltage at $(i+1)^{th}$ instant are subtracted with the values from $i^{th}$ instant.
vi. In the power voltage curve of the solar PV module, it is inferred that in the right-hand side curve where the voltage is almost constant and the slope of power voltage is negative ($\frac{\Delta P}{\Delta V} < 0$) whereas on the left-hand side, the slope is positive ($\frac{\Delta P}{\Delta V} > 0$). Therefore the right-hand side of the curve is for the lower duty cycle (nearer to zero) whereas the left-hand side curve is for the higher duty cycle (nearer to unity).
vii. Depending on the sign of ΔP which is P (i+1) – P (i) and ΔV which is V (i+1) –V (i) after subtraction the algorithm decides whether to increase the duty cycle or to reduce the duty cycle.

Then, flow charts of the P & O algorithm are as follows.

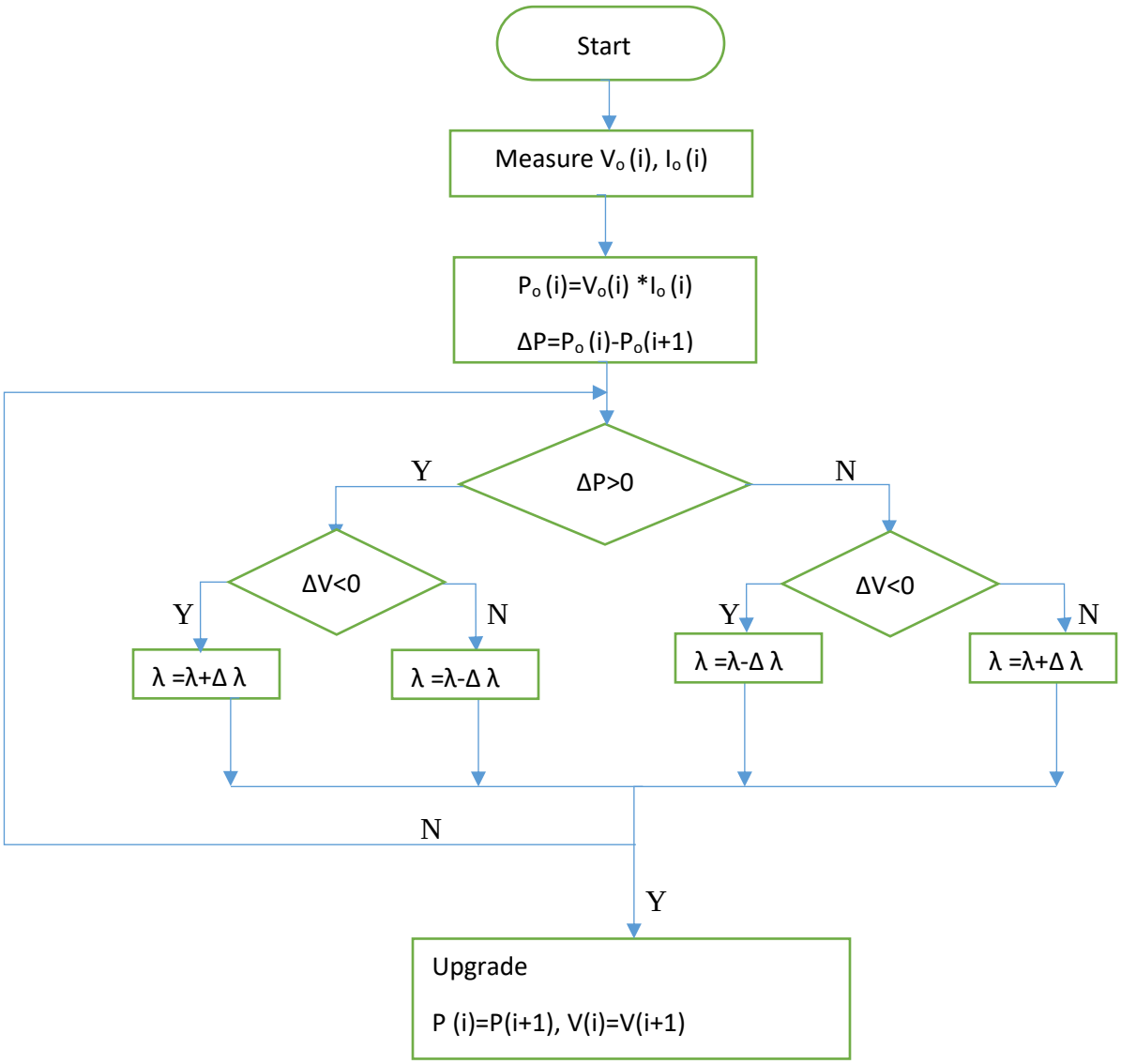


Figure 5. 1 P & O Algorithm

## 5.2. Inverter Control Strategies

Control strategies consist of PLL (phase-locked), DC Voltage regulator, a current regulator, and PWM modulator.

PLL is used to synchronize the grid with a PV array. Synchronization means the two sources having the same phase angle, frequency, and amplitude. In order to synchronize the grid with a PV array system single-phase PLL is used. It is a control system that provides a unity power factor by adjusting the phase of locally generated signal and the input signal. The objective of PLL in the grid-connected PV system is to synchronize grid voltage with inverter output voltage and the input of PLL is grid voltage and output that is the phase angle. Phase angle generated from PLL is used to generate the sine wave which acts as a reference signal to the PWM modulator control system [35].

Inverter control schemes

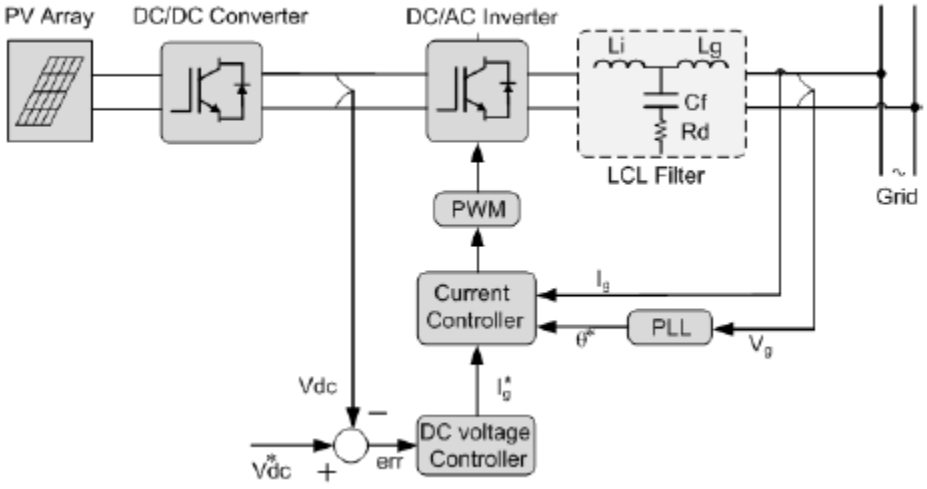


Figure 5. 2 Inverter control strategy

Phase-Locked Loop (PLL)

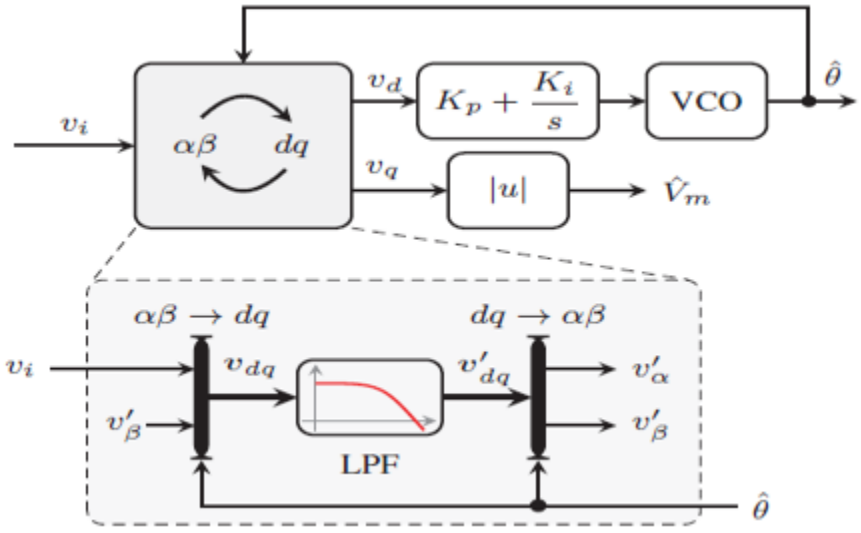


Figure 5. 3 Inverse park transform-based PLL

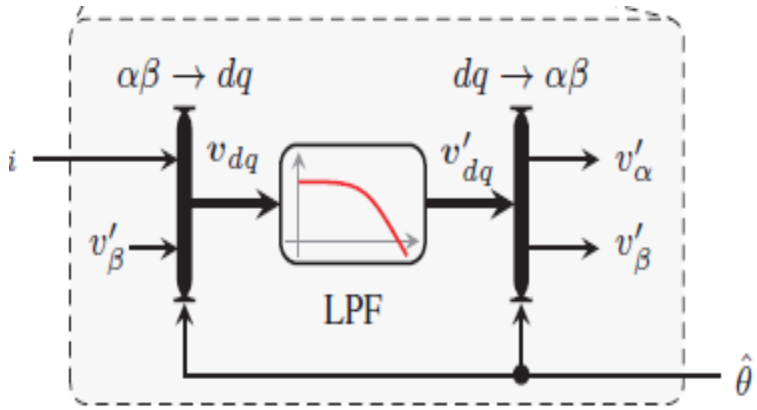


Figure 5. 4 Θ^ is a new generated phase angle

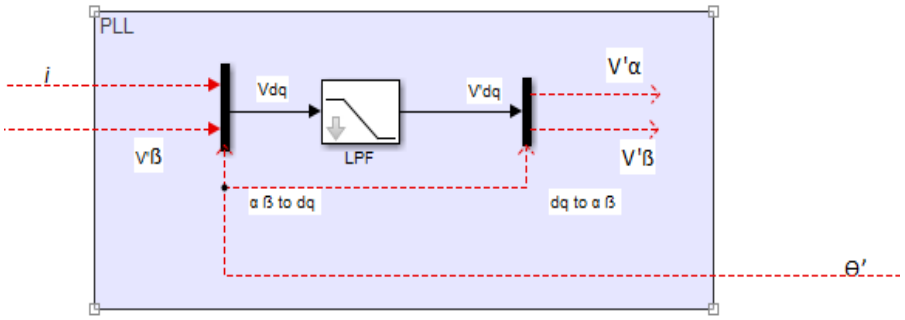


Figure 5. 5 PLL based grid-connected synchronization

Grid synchronization is an important issue in the grid-connected photovoltaic systems. Synchronization is based on the PLL techniques of inverse park transformation[36].

The PLL structure consists of a phase detector, a loop filter, and a voltage-controlled oscillator. If the loop filter is used as the first order low pass filter the small-signal model of a single-phase PLL will be a second-order system and the modeling of PLL is described as follows:

$$\frac{\theta o(s)}{\theta i(s)} = \frac{\mathrm{K1K2Gc(S)}}{S+K1K2Gc(S)} \qquad 5.1$$

Where: Gc(s) is the transfer function of the loop filter, K1 and K2 are the gains the phase detector and voltage-controlled oscillator. Gc(s) is while the PI controller forms the Ziegler Nicholas method.

$$Gc(s) = Kp + \frac{Ki}{S} \qquad 5.2$$

$$\frac{\theta o(s)}{\theta i(s)} = \frac{\mathrm{K1K2Kp\ S+K1K2Ki}}{S^2+K1K2Kp\ S+K1K2Ki} \qquad 5.3$$

Where: $\theta o$ is the output phase and $\theta i$ is the input phase.

Then, from the above transfer function, we can determine the damping natural frequency and damping ratio.

$$2\xi\omega n = K_1 K_2 K_p \quad 5.4$$

$$\omega n^2 = K_1 K_2 K_i \quad 5.5$$

Where: let $K_1 = K_2 = 1$

$$\xi = \frac{K_p}{2\sqrt{K_i}} \quad 5.6$$

$$\omega n = \sqrt{K_i} \quad 5.7$$

Again, the proportional gain can be determined $K_p$ and integral gain Ki by using Ziegler Nicholas tuning rules of PI controllers.

The PLL presented in this paper work is a single-phase PLL of inverse park transformation due to ease of implantation. The inverse park transform is DQ to α -ß can be used to generate output component 'ß' for orthogonal generator systems. While the input voltage is the 'α' component. Inverse park transformation of the PLL structure of the orthogonal signal generator is described by the following set of equations.

$$Vdq(s) = \begin{vmatrix} Vd(s) \\ Vq(s) \end{vmatrix} = Tp \begin{vmatrix} V'\alpha(s) \\ V'ß(s) \end{vmatrix} \quad 5.8$$

$$\text{V}\alpha\,ß\,(s) = \begin{vmatrix} V'\alpha\,(s) \\ V'\,ß\,(s) \end{vmatrix} = Tp^{-1} \begin{vmatrix} V'\text{d}(s) \\ V'\text{q}(s) \end{vmatrix} \quad 5.9$$

$$\begin{vmatrix} V'\text{d}(s) \\ V'\,\text{q}\,(s) \end{vmatrix} = G(s) \begin{vmatrix} V\text{d}\,(s) \\ V\text{q}\,(s) \end{vmatrix} = \frac{\omega\text{L}}{\text{S}+\omega\text{L}} \begin{vmatrix} V\text{d}(s) \\ V\text{q}(s) \end{vmatrix} \quad 5.10$$

Where: Tp is the park transformation matrix in the Laplace domain and G(s) is the low pass filter transfer function and ωL is cut-off frequency.

Park transformation of the single-phase signal is transformed into a two-phase signal and converted into the rotating frame by using the following relationships.

$$\begin{vmatrix} V\text{d} \\ V\text{q} \end{vmatrix} = \begin{vmatrix} \cos\Theta & sin\theta \\ -sin\theta & cos\theta \end{vmatrix} \begin{vmatrix} V\alpha \\ Vß \end{vmatrix} \quad 5.11$$

This transformation is used to generate an orthogonal signal generator in the single-phase structure[37], [38].

## 5.3. DC Voltage Regulator

DC voltage regulator is used to determine the required reference current for the current regulator from of phase angle of a phase-locked loop. PI controller is used to tuning the value of the proportional gain and integral gain of the controller. The value of proportional gain and integral gain are based on the trial and error method.

Current controller

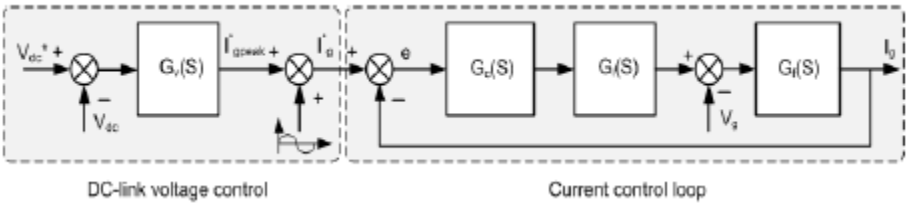


Figure 5. 6 Current and DC link voltage control schemes

In photovoltaic control schemes, the main important issue is to control the load current. To control this load current the conventional PI controller is used. The Proportional and integral gain of the controller is estimated by using Ziegler Nichols rules by setting initially Ti=∞ and Td=0 and by increasing Kp from zero to the critical value we can get sustained the oscillations.

Then,

$$Gc(S)= K_p+K_i/s =K_p(1+1/T_iS) \quad 5.12$$

Where $T_i$ will be expressed by the following equation:

$$T_i=K_p/K_i \quad 5.13$$

According to Ziegler Nichols tuning method, the value of gains can be estimated as follows:

$K_p=0.45Kcr$ and $T_i=1/1.2P_{cr}$.

Where critical period Pcr also expressed as follows :

$$P_{cr}=2\pi/\omega \quad 5.14$$

The value of ω can be calculated by substituting jω into S of S domain characteristic equations of the transfer function.

Then, the input to output relationship of the current regulator is modeled as follows:

$$Ig=H_i(S)I'_g - H_g(S)V_g \quad 5.15$$

Where: $H_i(S)$ is the transfer function of Ig to $I'_g$, $H_g(S)$ is the transfer function of Ig to Vg, Ig is grid current, Vg is grid voltage and $I'_g$ is reference current.

Then, $H_i(S)$ and $H_g(S)$ is given as follows:

$$Hi(S) = \frac{Gc(S)*Gi(S)*Gf(S)}{1+Gc(S)*Gi(S)*Gf(S)} = \frac{Ig}{I'g} \quad 5.16$$

$$Hg(S) = \frac{Gf(S)}{1+Gc(S)*Gi(S)*Gf(S)} = \frac{Ig}{Vg} \quad 5.17$$

Where: $Gf(S)$ is the transfer function of LCL filter, Gc(S) is T.F of PI controller and Gi(S) is T.F of Inverter which is constant K.

Then,

$$Gf(S) = \frac{RCS+1}{LiLgCS^3+(Li+Lg)RCS^2+(Li+Lg)S} \quad 5.18$$

# Chapter Six

# 6. Results, Conclusions, and Recommendation

## 6.1. Results

In this thesis work, the assessment of a grid-connected solar PV system is analyzed, designed, and simulated for traction application of train. Before designing and simulation of the grid-connected photovoltaic system in the MATLAB/Simulink solar radiation of the location should be estimated and studied. The feasibility of the site is also analyzed. Solar radiation of the site is dependent on the sun, altitude, maximum and minimum temperature of the site, type of solar module, and numbers of solar cells and efficiency. In this thesis work monocrystalline solar panel with the wattage of 345W and area of the module is 1.94 $m^2$ is used. Solar panel with this specification is available in the local market. The rest of the components are not available in the local market like that of 100 kVA inverter and DC to DC (Boost) converter used for high power applications due to that of large scale power generation from the PV system is not adopted in the country for the past years but, those components are available in the international market. The average solar radiation of the Adama, Metehara, Awash Arba, and Asebe Teferi site is computed and listed in the table above from Table 3.3 to Table 3.6. The results are estimated by using the most know formula of temperature-based estimation of solar radiation and show's the great result to generate power from the PV system. The average solar radiation obtained from each site is as follows: 6.62 $kWh/m^2$, 7.26 $kWh/m^2$, 6.891 $kWh/m^2$ and 6.45 $kWh/m^2$ are for Adama, Metehara, Awash Arba (7), and Asebe Teferi respectively.

The simulation results after the first 0.5 seconds the generated output power is almost to 1MW with almost zero reactive power. Another thing that is analyzed in this thesis is feasibility and carbon dioxide emission reduction by using a PV system. The feasibility of the designed PV system is studied and it takes only 5 years which shows that the designed system is feasible and it saves 124980.44 tons of Co2 throughout the lifetime of the project. For a single-phase grid-connected PV system the circuit designed in the MATLAB and simulation results is given below.

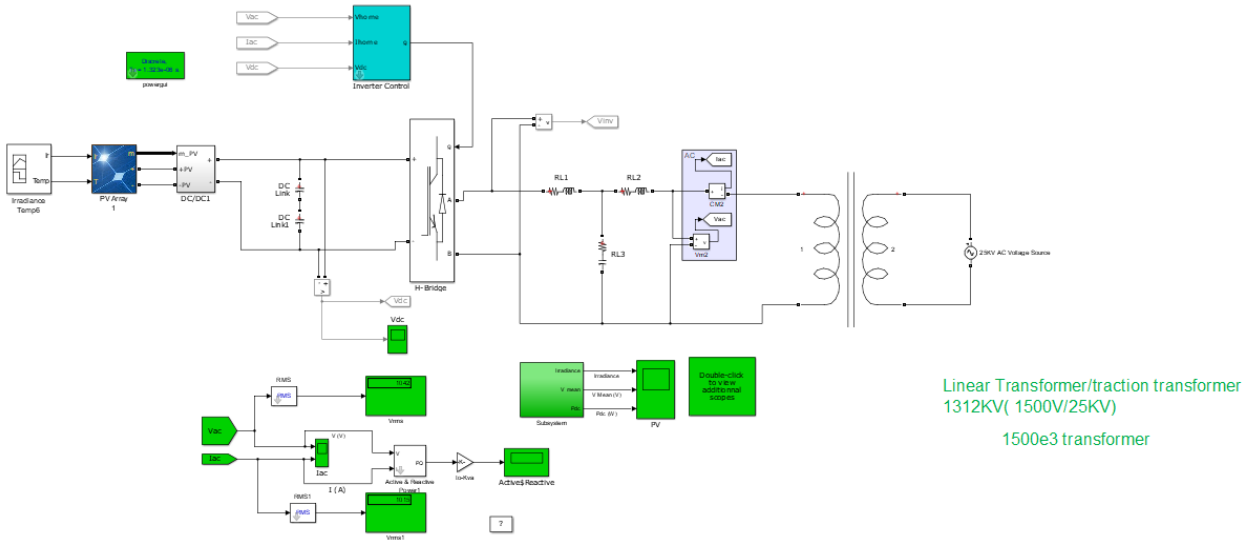


Figure 6. 1 MATLAB design for single-phase PV grid-connected system

The output of the MATLAB simulation is PV array output ($V_{pv}$ and $P_{DC}$), DC link voltage, $V_{inv}$, AC output voltage, and current and active and reactive powers.

PV array output voltage from simulation result is around 640 V DC and output DC power is which 1MW. DC link output voltage is 1600 V with having duty cycle the 0.6, the inverter output voltage is also 1600 V AC so, from simulation results active and reactive power are approximately 1MW and zero reactive power (0 KVAR) which shows is excellent results.

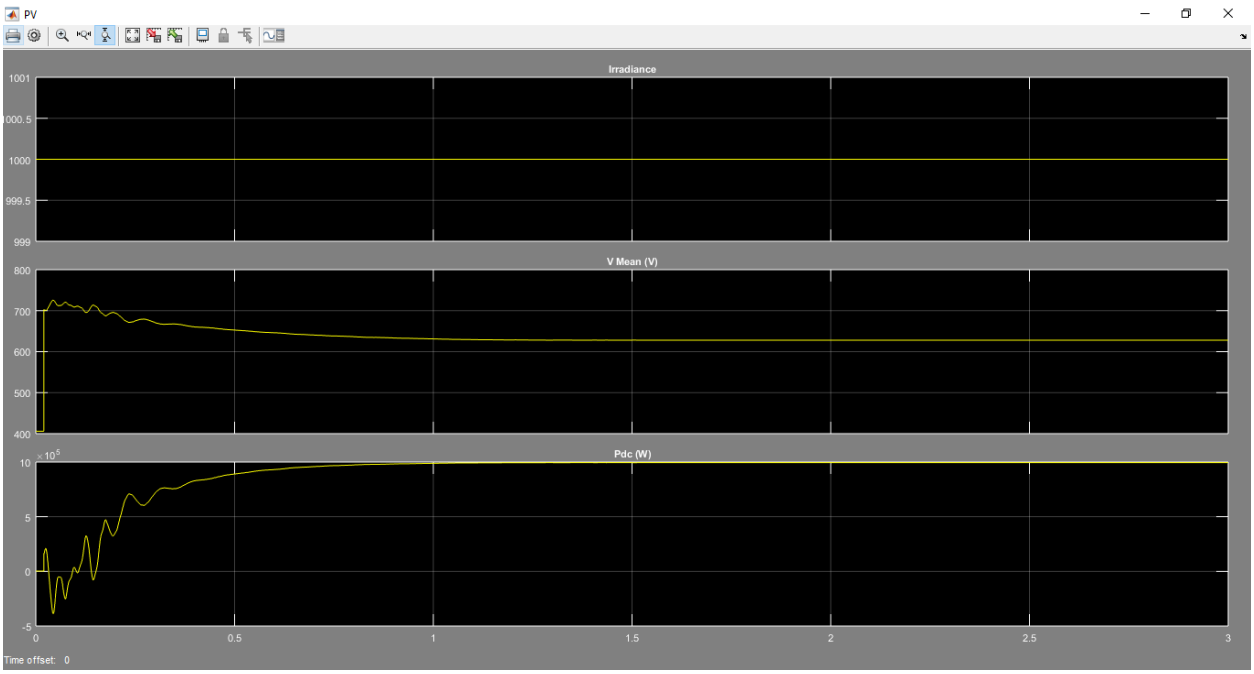


Figure 6. 2 Irradiance, PV array output voltage, and output DC power

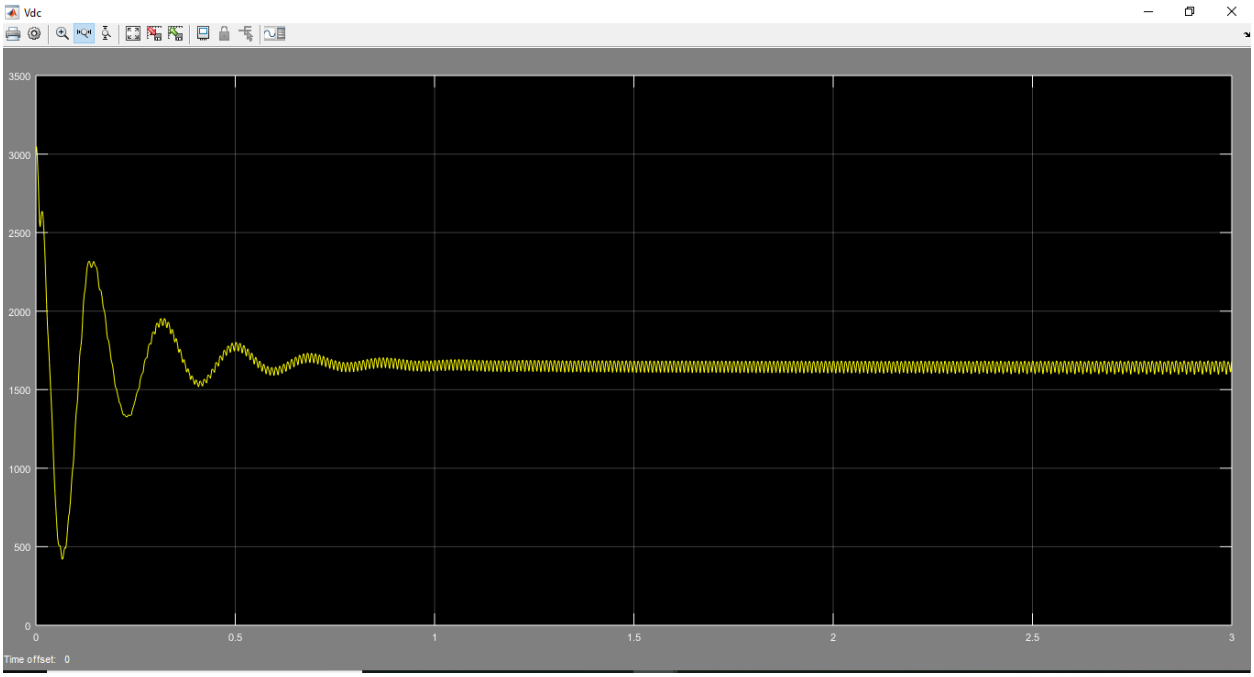


Figure 6. 3 DC-Link voltage

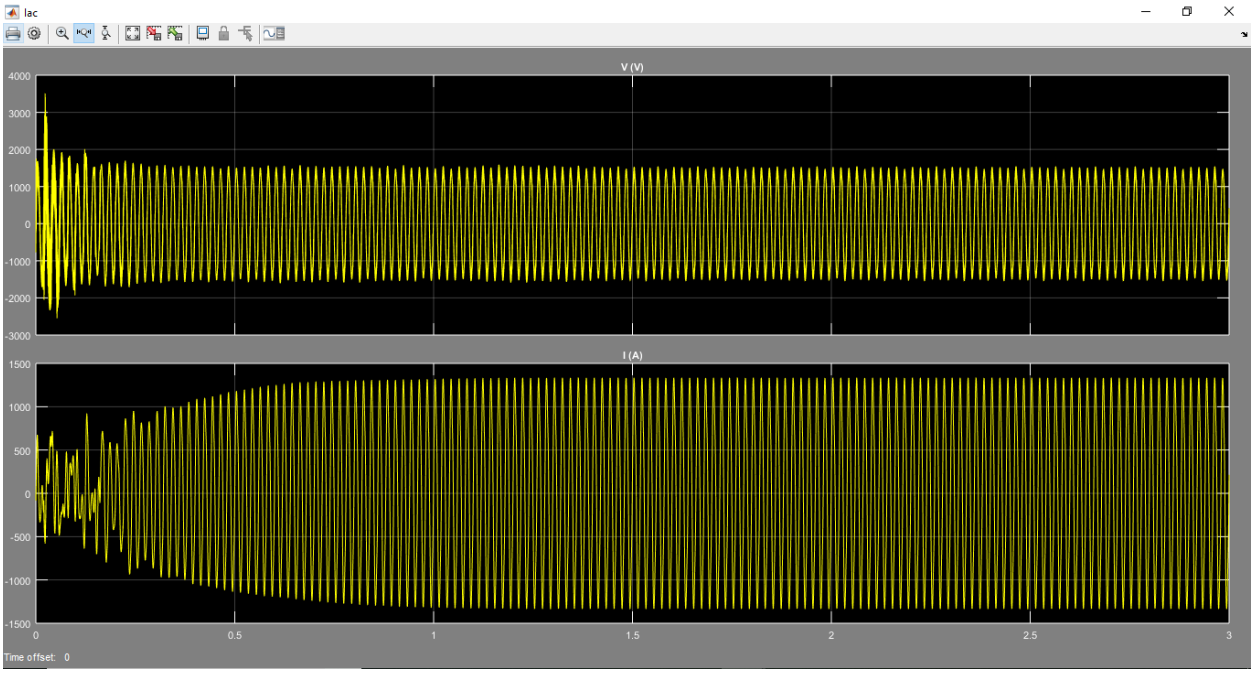


Figure 6. 4 Inverter voltage and current

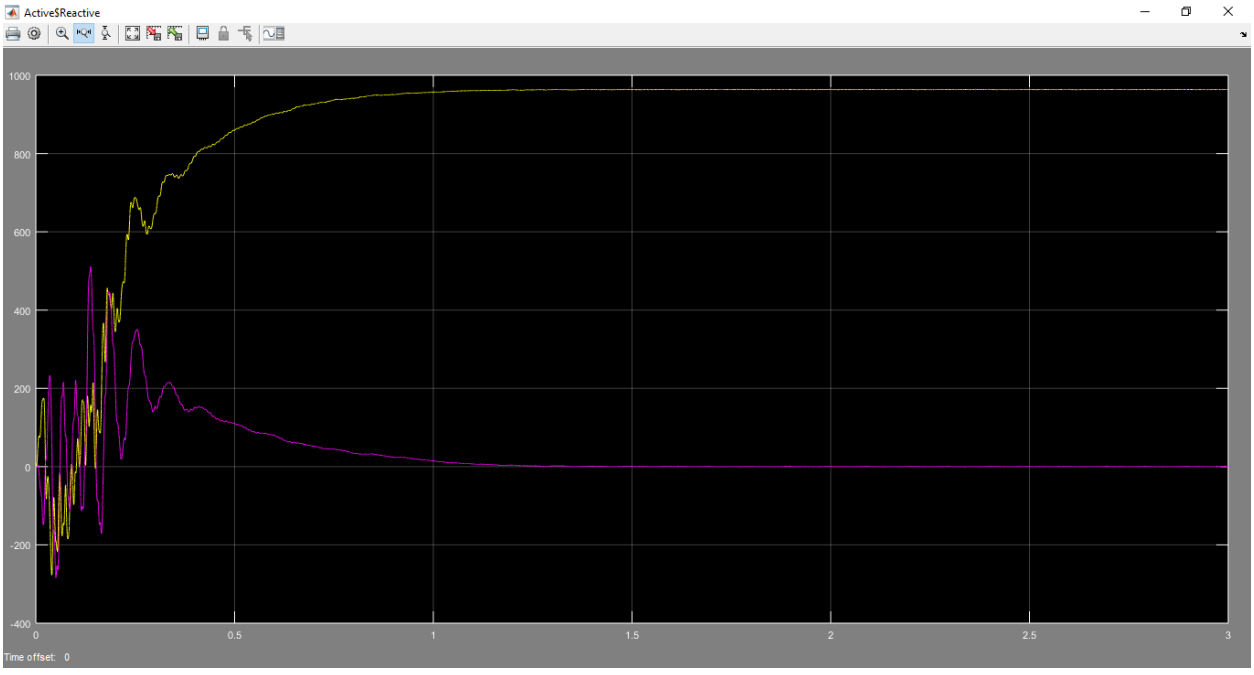


Figure 6. 5 Active and reactive power of the grid-connected PV system

## 6.2. Conclusions

Ethiopia is found near to equator at a latitude of 8 degrees north and longitude of 38 degrees east having the high solar potential to generate power.

In this thesis work, average global solar radiation, feasibility, payback, carbon dioxide emission, and design and simulation of the grid-connected photovoltaic system is done. In chapter three and chapter four all analysis and design and simulation of the grid-connected solar photovoltaic system are studied.

To analyze the feasibility of the site solar radiation is determined by using well know temperature model method. Meteorological data is collected from National Meteorological Agency then, from the analysis, the system is feasible which means obtained solar radiation of the site is more than an international standard to generate power from the solar photovoltaic system. From the analysis of the above chapters the obtained average global solar radiation is greater than 6 $kWh/m^2/day$. The energy computed from the solar system is 28,534.35 kWh/day and 10,415,036.48 kWh/yearly then, the feasibility of the system is analyzed and which takes 5 years throughout the lifetime of the project. Another thing studied in this thesis work is a payback of the invested capital cost which is from analysis results it takes five years. Under here carbon dioxide emission is also studied well and saves 124,980.44 tons of $Co_2$ through a lifetime of the systems. Using the solar photovoltaic system is a great contribution to the green economy. The system used for this thesis is a single-phase grid-connected photovoltaic system. Design and simulation of the system are by using MATLAB/Simulink as sensitive tools and integration of the system is shown by using these sensitive tools.

Then, in the end, it is possible to conclude that the generated power from the solar photovoltaic system in the Ethio-Djibouti route is more than enough to accommodate train and auxiliary loads.

## 6.3. Recommendation

In this thesis study, the single-phase grid-connected photovoltaic system is considered and the design and simulation of the system are simulated in a good manner. If the government appreciate either local or international solar system supplier it is helpful for the green economy as well as to reduce power interruption for our trainloads or in our country. There is big problem with data on the new due to project is on going and even there is also officer problem here and there to get at least sufficient datas.

## 6.4. Future Work

Since this thesis is done with remaining problems which are further studied. The thesis may be studied and enlarged with the following points:

1. Environmental conditions of the site because wind speed and dust conditions are not considered in my study to install the PV system in the site.
2. Daily energy consumption of train load under full operation for the new upcoming Ethio-Djibouti rail route.
3. The space needed to install photovoltaic to generate power from a photovoltaic system.
4. The measured meteorological data for the selected site.
5. Analyzing the behavior of a single-phase photovoltaic system for big loads.

## REFERENCE


[1] J. A. Duffie, W.A. Beckman "Solar Engineering of the thermal process,"2013.

[2] T. Eth, "About EEPC 2001," 2008.

[3] M. G. Villalva, J. R. Gazoli, and E. F. Ruppert, "MODELING AND CIRCUIT-BASED SIMULATION OF PHOTOVOLTAIC ARRAYS," vol. 14, no. 1, 2009.

[4] M. Unibertsitatea, L. Abrahamsson, and J. Sanz, "Electrical railway power supply systems : current situation and future trends," no. November, 2017.

[5] S. R. Kumar, K.V. Gaikwad, and M.A. Surya, "COURSE ON THREE PHASE TECHNOLOGY."

[6] N. L. Tirupathamma, M. Rajesh, K. N. Vamsi, R. Lohitha, and P. Sravan, "Matlab Simulation of Grid Connected PV System Using Hysteresis Current Control Inverter," vol. 4840, no. 5, pp. 13–20, 2014.

[7] E. Quansah, L. K. Amekudzi, K. Preko, J. Aryee, O. R. Boakye, D. Boli, and M. R. Salifu, "Empirical Models for Estimating Global Solar Radiation over the Ashanti Region of Ghana," vol. 2014, pp. 9–12, 2014.

[8] A. Javier, B. Monica, and W. Enrique, " Estimation of daily global solar radiation from measered temepratures at Canada de Luque, Cordoba, Argentina,"2013.

[9] A. Q. Jakhrani, A. K. Othman, A. R. H. Rigit, and S. R. Samo, "A simple method for the estimation of global solar radiation from sunshine hours and other meteorological parameters," 2010.

[10] N. Argaw, "Estimation of solar radiation energy of ethiopia from sunshine data," *Int. J. Sol. Energy*, vol. 18, no. 2, pp. 103–113, 1996.

[11] S. A. Mekonnen, "SOLAR ENERGY ASSESSMENT IN ETHIOPIA : MODELING AND MEASUREMENT," no. July, 2007.

[12] S. Kebede, "DESIGN OF HYBRID SOLAR ENERGY SYSTEM FOR THE APPLICATION OF TRAIN LOCOMOTIVE POWER SOURCE FOR THE AALRT

AND ETHIO-DJIBOUTI ROUTS," no. March, 2015.

[13] P. Engineering and S. Pes, "Performance Analysis of Grid Connected Solar PV System Using Matlab / Simulink," vol. 3, no. September, pp. 48–54, 2013.

[14] R. Verma and P. K. Gupta, "Simulation of grid connected photovoltaic system using MATLAB / Simulink," no. 6, pp. 669–674, 2017.

[15] M. S.Hassan and A. A. Elbaset, "A Comparative Study for Optimum Design of Grid Connected PV System based on Actual System Specifications," *Int. J. Comput. Appl.*, vol. 116, no. 3, pp. 19–34, 2015.

[16] J. Abdulateef, "Simulation of solar off- grid photovoltaic system for residential unit," vol. 4, pp. 29–33, 2014.

[17] C. Wai, K. Louis, and R. A. Gambol, "Estimation of Global Solar Radiation from Meteorological Parameter in Peninsular Malaysia," no. 3, pp. 1–2, 2014.

[18] "citation-262559454." .

[19] M. S. Hassan and A. A. Elbaset, "A Comparative Study for Optimum Design of Grid Connected PV System based on Actual System Specifications," vol. 116, no. 3, pp. 19–34, 2015.

[20] T. Power and F. Ciccarelli, "Integration of Photovoltaic Plants and," pp. 1–14, 2018.

[21] D. Gowda, S. S. Lokare, N. N. Kumbhar, B. Kolekar, and A. K. Teli, "MODIFICATIONS OF SOLAR TRAIN," vol. 7, no. 3, pp. 434–444, 2018.

[22] M. S. Vasisht, G. A. Vashista, J. Srinivasan, and S. K. Ramasesha, "Rail coaches with rooftop solar photovoltaic systems : A feasibility study Rail coaches with rooftop solar photovoltaic systems : A feasibility study," *Energy*, no. January 2018, 2017.

[23] D. O. Akpootu and Y. A. Sanusi, "A New Temperature-Based Model for Estimating Global Solar Radiation in Port-Harcourt , South-South Nigeria .," no. 2004, pp. 63–73, 2015.

[24] M. I. Al-najideen and S. S. Alrwashdeh, "Resource-Efficient Technologies Design of a solar photovoltaic system to cover the electricity demand for the faculty of Engineering-Mu ' tah University in Jordan," *Resour. Technol.*, vol. 3, no. 4, pp. 440–445, 2020.

[25] C. S. Engineering, "Faculty of Graduate Studies Design and Simulation of a Photovoltaic System with Maximum Power Control to Supply a Load with Alternating Current By,"

2012.

[26] L. Fara, D. Craciunescu, "Output Analysis of Stand-Alone PV Systems: Modeling, Simulation and Control," *Energy Procedia 112, 595 – 605* October 2017.

[27] A. Shaw, "Grid-connected PV systems design guidelines for the pacific islands" 2012.

[28] A. N. Al-shamani, M. Yusof, H. Othman, S. Mat, M. H. Ruslan, A. M. Abed, and K. Sopian, "Design & Sizing of Stand-alone Solar Power Systems A house Iraq," pp. 145–150.

[29] S. Sumathi, *Application of MATLAB / SIMULINK in Solar PV Systems*," 2015.

[30] M. Hammad, M. S. Y. Ebaid, G. Halaseh, and B. Erekat, "Large Scale Grid Connected ( 20MW ) Photovoltaic System for Peak Load Shaving in Sahab Industrial District," vol. 9, no. 1, pp. 45–59, 2015.

[31] A. A. A. Al-khazzar, "The Required Land Area for Installing a Photovoltaic Power Plant," *Iran. J. Energy Environ.*, no. April, pp. 11–18, 2017.

[32] S. M. A. Faisal, "Model of Grid Connected Photovoltaic System Using MATLAB / SIMULINK," pp. 1–12.

[33] V. P. Sector, "Solar Photovoltaics," vol. 1, no. 4, 2012.

[34] K. Dubey, "DESIGN AND SIMULATION OF SOLAR PV," pp. 568–573, 2016.

[35] D. Version, "Aalborg Universitet Synchronization in single-phase grid-connected photovoltaic systems under grid faults Synchronization in Single-Phase Grid-Connected Photovoltaic Systems under Grid Faults," 2012.

[36] K. Arun and K. Selvajyothi, "Observer Based Current Controlled Single Phase Grid Connected Inverter," *Procedia Eng.*, vol. 64, pp. 367–376, 2013.

[37] L. Shilpa, P. Anu, R. Divya, and M. G. Nair, "Single Phase D-Q Theory Based Control of DER Inverters for Power Quality Improvement," pp. 170–176, 2015.